

Numerical Methods III: Review of vertical coordinates and vertical discretizations

Michael Toy

Department of Atmospheric Science

Colorado State University

August 1, 2012



Outline

- Introduction
- Vertical coordinates
 - Overview of coordinate systems
 - Terrain-following variations
- Vertical discretizations
 - Hydrostatic relation
 - Computational modes
 - Accuracy of normal modes
- Quasi-Lagrangian coordinates

Unique aspects of the vertical dimension

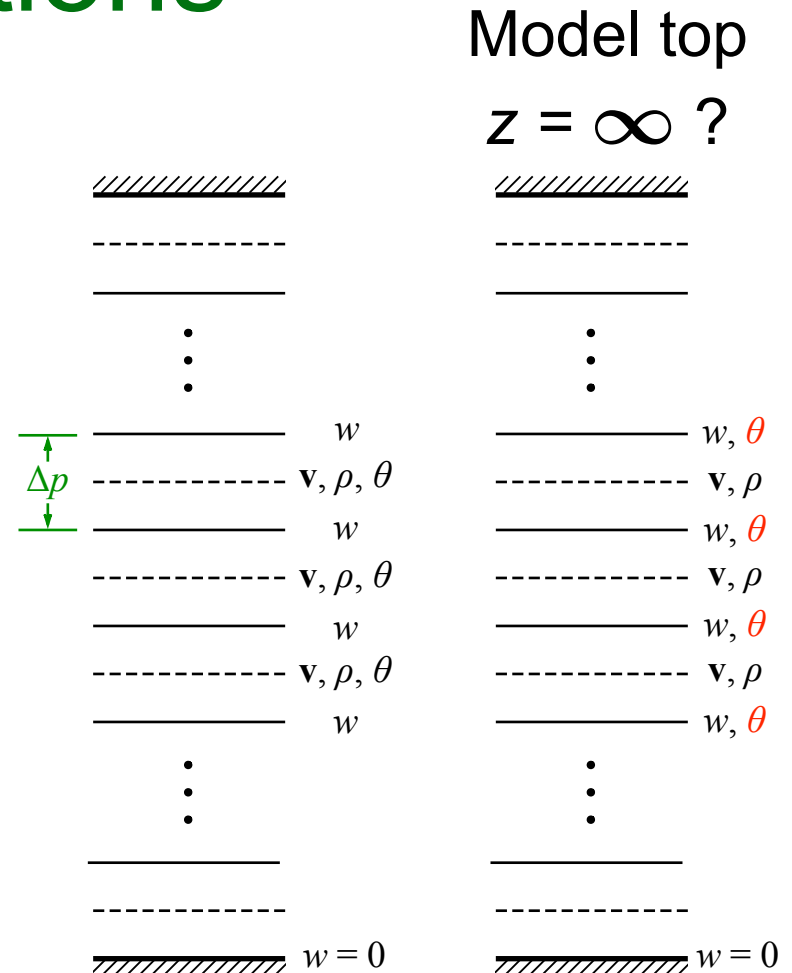
- Gravity acts along it
 - Atmosphere highly stratified
 - Vertical motion somewhat suppressed
- Gradients much stronger in the vertical
 - It's much colder 10 km straight up (-50 C, and harder to breathe) than it is 10 km down the road
- Boundary conditions at $z = z_{surface}$ and $z = \infty$
- Many different coordinate systems used to measure it

Unique aspects of the vertical dimension

- Distinct processes
 - Convection
 - Boundary layer (and interaction with free atmosphere)
 - Radiation
 - Waves

Unique aspects of vertical discretizations

- There's always work to do
 - i.e., hydrostatic relation must be satisfied for a motionless atmosphere
- Staggering considerations
- Boundary conditions



Various vertical coordinates used in atmospheric models



z



Richardson
(1922)

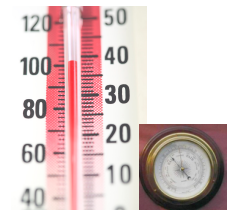
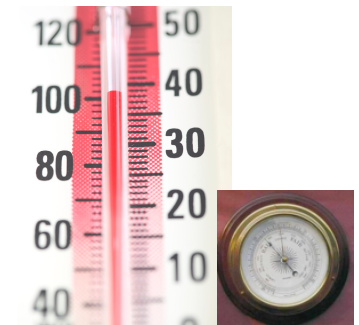
p



π



θ



Eliassen
(1949)

Laprise
(1992)

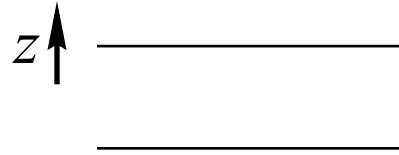
Eliassen & Raustein
(1968)

z-coordinates

Nonhydrostatic
dynamical cores

5 prognostic variables/equations

$$\frac{D\mathbf{v}}{Dt} + f \mathbf{k} \times \mathbf{v} = -\frac{1}{\rho} \nabla_z p \quad \text{Horizontal momentum}$$



$$\frac{Dw}{Dt} = -\frac{1}{\rho} \frac{\partial p}{\partial z} - g \quad \text{Vertical momentum}$$

$$\left(\frac{\partial \rho}{\partial t} \right)_z + \nabla_z \cdot (\rho \mathbf{v}) + \frac{\partial}{\partial z} (\rho w) = 0 \quad \text{Mass continuity}$$

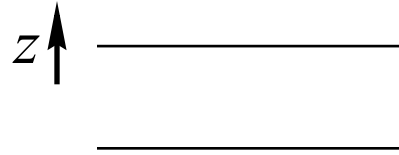
$$\frac{D\theta}{Dt} = \frac{Q}{\Pi} \quad \text{Thermodynamics}$$

z-coordinates

Hydrostatic
dynamical cores

4 prognostic variables/equations

$$\frac{D\mathbf{v}}{Dt} + f \mathbf{k} \times \mathbf{v} = -\frac{1}{\rho} \nabla_z p \quad \text{Horizontal momentum}$$



$$0 = -\frac{1}{\rho} \frac{\partial p}{\partial z} - g \quad \text{Hydrostatic relation}$$

$$\left(\frac{\partial \rho}{\partial t} \right)_z + \nabla_z \cdot (\rho \mathbf{v}) + \frac{\partial}{\partial z} (\rho w) = 0 \quad \text{Mass continuity}$$

$$\frac{D\theta}{Dt} = \frac{Q}{\Pi} \quad \text{Thermodynamics}$$

z-coordinates

Computing the vertical velocity

$$w \equiv \frac{Dz}{Dt}$$

Nonhydrostatic
dynamical cores

vs.

Hydrostatic
dynamical cores

Predicted

$$\frac{Dw}{Dt} = -\frac{1}{\rho} \frac{\partial p}{\partial z} - g$$

$$w = -\int_0^z \nabla \cdot \mathbf{v} dz - \frac{1}{\gamma} \int_0^z \frac{1}{p} (B + J) dz + \frac{1}{c_p} \int_0^z \frac{Q}{T} dz$$

Diagnosed

- Hydrostatic DC's rarely use z-coordinates due to difficulty of w diagnosis.

- Examples:
Kasahara and Washington (1967)
DeMaria (1995)

where

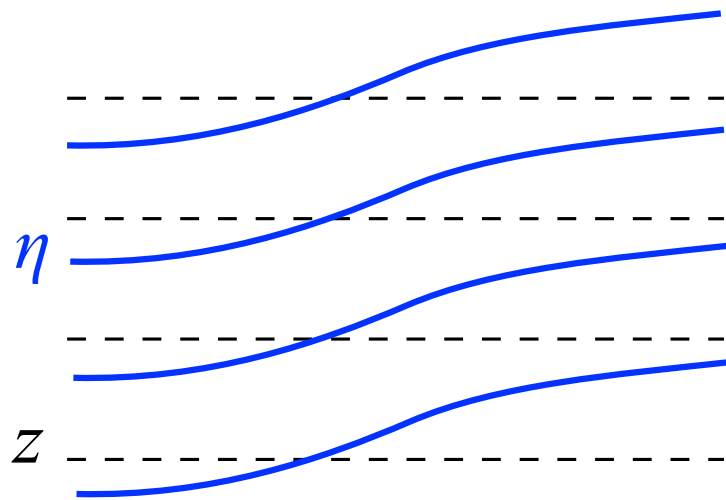
$$B = \frac{\frac{1}{\gamma} \int_0^{z_T} \frac{J}{p} dz - \frac{1}{c_p} \int_0^{z_T} \frac{Q}{T} dz + \int_0^{z_T} \nabla \cdot \mathbf{v} dz}{-\frac{1}{\gamma} \int_0^{z_T} \frac{dz}{p}}$$

$$J = \mathbf{v} \cdot \nabla p - g \int_z^{z_T} \nabla \cdot (\rho \mathbf{v}) dz$$

Richardson's equation

Vertical coordinate transformations

$$\eta(x, y, z, t) \rightarrow z(x, y, \eta, t)$$



Transformation rules:

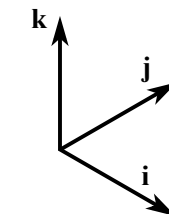
$$\frac{\partial}{\partial z} = \frac{\partial \eta}{\partial z} \frac{\partial}{\partial \eta}$$

$$\left(\frac{\partial}{\partial t} \right)_z = \left(\frac{\partial}{\partial t} \right)_\eta - \left(\frac{\partial z}{\partial t} \right)_\eta \frac{\partial \eta}{\partial z} \frac{\partial}{\partial \eta}$$

$$\nabla_z = \nabla_\eta - \nabla_\eta z \frac{\partial \eta}{\partial z} \frac{\partial}{\partial \eta}$$

Generalized vertical velocity: $\dot{\eta} = \frac{D\eta}{Dt} = \left(\frac{\partial \eta}{\partial t} \right)_z + \mathbf{v} \cdot \nabla_z \eta + w \frac{\partial \eta}{\partial z}$

Note: Usual velocity components (u, v, w)
retained as well as unit coordinate vectors $\mathbf{i}, \mathbf{j}, \mathbf{k}$



Compressible Euler equations in a generalized vertical coordinate (η)

6 prognostic variables/equations

$$\frac{D\mathbf{v}}{Dt} + f \mathbf{k} \times \mathbf{v} = -\frac{1}{\rho} \nabla_{\eta} p + \frac{1}{m} \frac{\partial p}{\partial \eta} \nabla_{\eta} z$$

Horizontal momentum

$$\frac{Dw}{Dt} = -\frac{1}{m} \frac{\partial p}{\partial \eta} - g$$

2-term horiz.
pressure
gradient !!!

Vertical momentum

$$\left(\frac{\partial m}{\partial t} \right)_{\eta} + \nabla_{\eta} \cdot (m\mathbf{v}) + \frac{\partial}{\partial \eta} (m\dot{\eta}) = 0$$

$$m = \rho \frac{\partial z}{\partial \eta}$$

Mass continuity

$$\frac{D\theta}{Dt} = \frac{Q}{\Pi}$$

new mass variable
(pseudo-density)

Thermodynamics

$$\frac{Dz}{Dt} = w$$

z is predicted

Geopotential height
prediction

Pressure coordinates

$$\eta = p$$

Nonhydrostatic
dynamical cores

vs.

Hydrostatic
dynamical cores

$$\frac{Dw}{Dt} = -\frac{1}{m} - g$$

single-term
HPGF

$$\frac{D\mathbf{v}}{Dt} + f \mathbf{k} \times \mathbf{v} = \frac{1}{m} \nabla_p z$$

Vertical momentum
mass is a constant

$$m = -\frac{1}{g}$$

single-term
HPGF

$$\frac{D\mathbf{v}}{Dt} + f \mathbf{k} \times \mathbf{v} = -g \nabla_p z$$

$$\left(\frac{\partial m}{\partial t} \right)_p + \nabla_p \cdot (m\mathbf{v}) + \frac{\partial}{\partial p} (m\omega) = 0$$

Continuity

Vertical velocity ω
difficult to diagnose

diagnostic
continuity

$$\nabla_p \cdot \mathbf{v} + \frac{\partial \omega}{\partial p} = 0$$

Vertical velocity
easily diagnosed

$$\omega \equiv \dot{p} = - \int \nabla_p \cdot \mathbf{v} dp$$

Hydrostatic pressure (a.k.a. mass) coordinates

$$\eta = \pi$$

$$\pi(x, y, z, t) = \int_z^{\infty} \rho(x, y, z', t) g dz'$$

- i.e., the mass of air above a given height
- For a hydrostatically balanced atmosphere, this is the pressure p
- Whether hydrostatic or not, this gives
 - a pseudo-density of constant value $m = \rho dz/d\pi = -g^{-1}$
 - a diagnostic continuity equation $\nabla_{\pi} \cdot \mathbf{v} + \frac{\partial \dot{\pi}}{\partial \pi} = 0$
 - a vertical velocity which is easily diagnosed as $\dot{\pi} = - \int \nabla_{\pi} \cdot \mathbf{v} d\pi$

ISENTROPIC COORDINATES

$$\eta = \theta$$

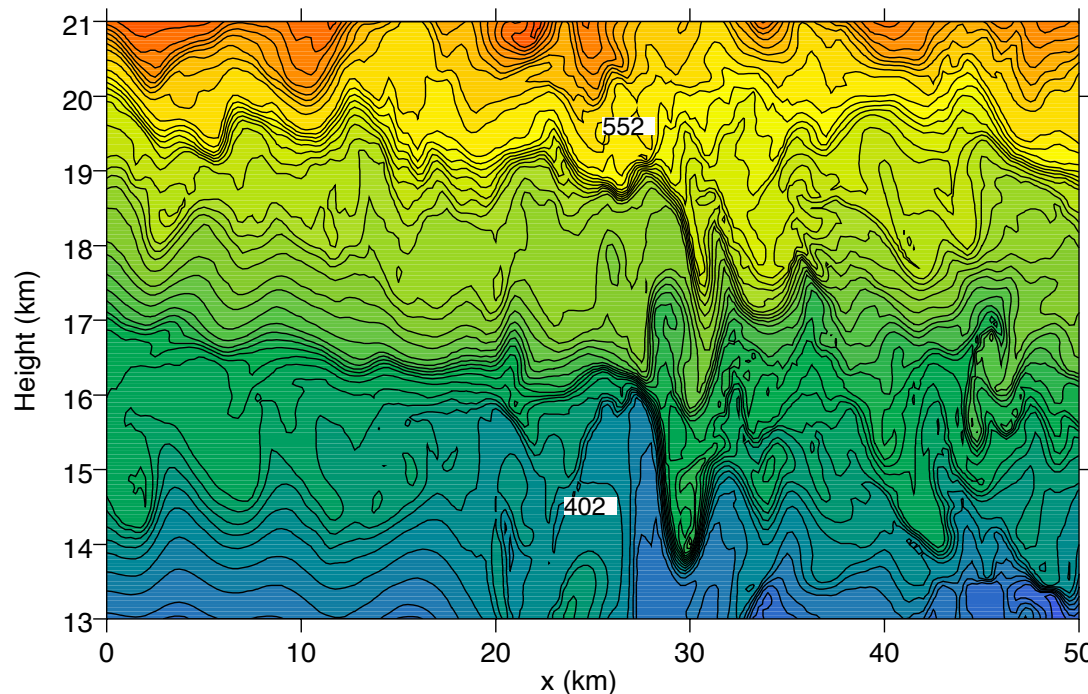
$$\theta = c_p \frac{T}{\Pi} \quad \text{where} \quad \Pi = c_p \left(\frac{p}{p_0} \right)^{R/c_p} \quad (\text{Exner function})$$

- The vertical velocity is proportional to the diabatic heating $\dot{\theta} \equiv \frac{D\theta}{Dt} = \frac{Q}{\Pi}$
- For an adiabatic atmosphere, the “vertical motion” is zero and coordinate surfaces are material surfaces (a quasi-Lagrangian vertical coordinate)
 - This minimizes the error associated with vertical advection
- Ertel’s potential vorticity can be explicitly represented as the model winds lie along isentropic surfaces
- Wave momentum transport occurs via isentropic form drag as opposed to eddy fluxes

ISENTROPIC COORDINATES

$$\eta = \theta$$

- In nonhydrostatic models and high horizontal resolution, negative static stabilities and turbulence present a challenge (more on this later)



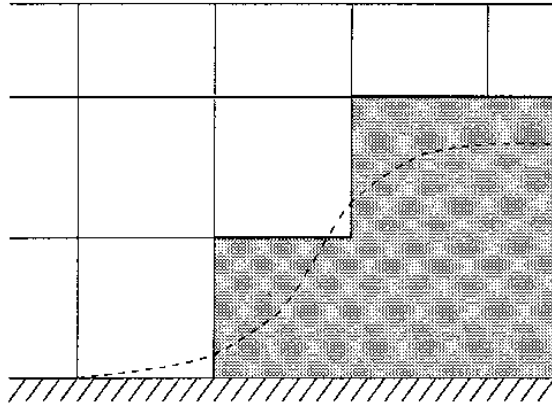
Vertical cross-section of isentropes
associated with a breaking mountain wave

Summary of vertical coordinate overview

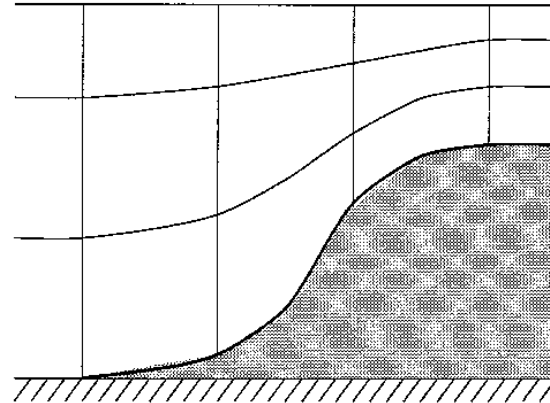
	Nonhydrostatic models	Hydrostatic models
z coordinate	Suitable	Not preferred (difficulty in diagnosing w)
p coordinate	Not preferred (difficulty in diagnosing ω)	Suitable
π (mass) coordinate	Suitable	Suitable (identical to p -coordinate)
θ coordinate	Suitable (challenges with fine-scale turbulent flow)	Suitable

Representation of topography

a) Step topography



b) σ -coordinates



c) Shaved cell

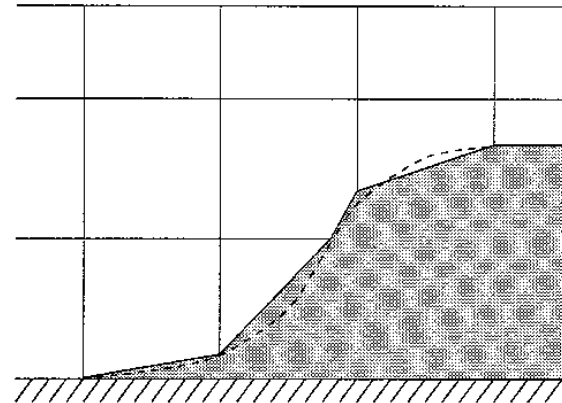


FIG. 1. The representation of a smoothly varying bottom (dashed line) in (a) a height coordinate model using step topography, (b) a terrain-following coordinate model, and (c) a height coordinate model with piecewise constant slopes.

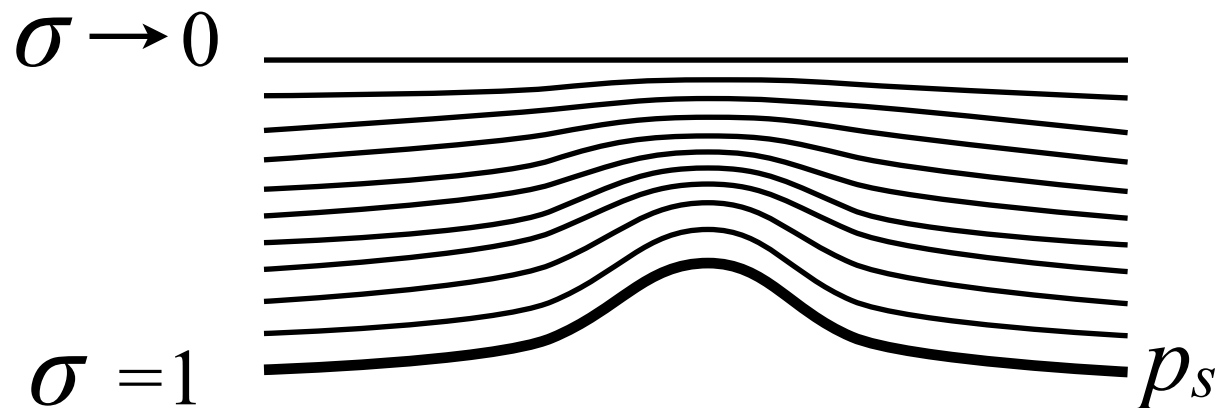
Shaved (or “cut”) cell methods are emerging, e.g.,

- Adcroft et al. (1997)
- Steppeler et al. (2002) (DWD Lokal-Modell)
- Walko and Avissar (2008) (OLAM model)
- Yamazaki and Satomura (2010)
- Lock et al. (2012)

Figure from Adcroft et al. (1997)

Terrain-following (σ) coordinates

$$\sigma \equiv \frac{p}{p_s} \quad \text{Phillips (1957)}$$



Advantages:

- Lower boundary is a coordinate surface
- Simple lower boundary condition -- $(\dot{p})_{\sigma=1} = 0$

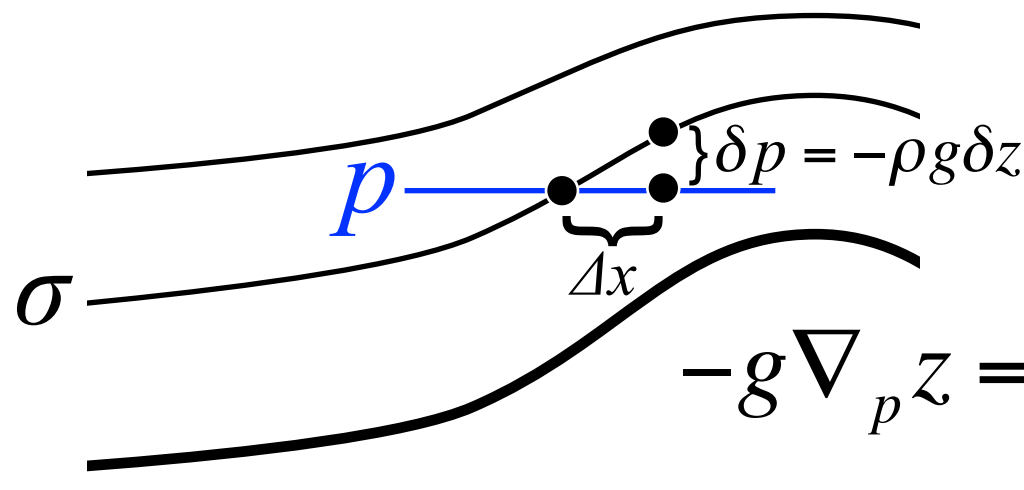
Disadvantage:

- Large discretization error in horizontal pressure gradient force for steep topography

$$-g \nabla_p z = -g \nabla_\sigma z - \frac{1}{\rho} \nabla_\sigma p$$

Terrain-following (σ) coordinates

$$\sigma \equiv \frac{p}{p_s}$$



$$-g \nabla_p z = 0 = -g \nabla_\sigma z - \frac{1}{\rho} \nabla_\sigma p$$

$$0 \approx -g \nabla_\sigma z - \frac{1}{\rho} \nabla_\sigma p$$

The discrete forms of these terms don't necessarily cancel



Terrain-following (σ) coordinates

For more information on the horizontal pressure gradient force error and how to reduce spurious motions and satisfy various integral constraints (e.g., angular momentum and total energy conservation), see:

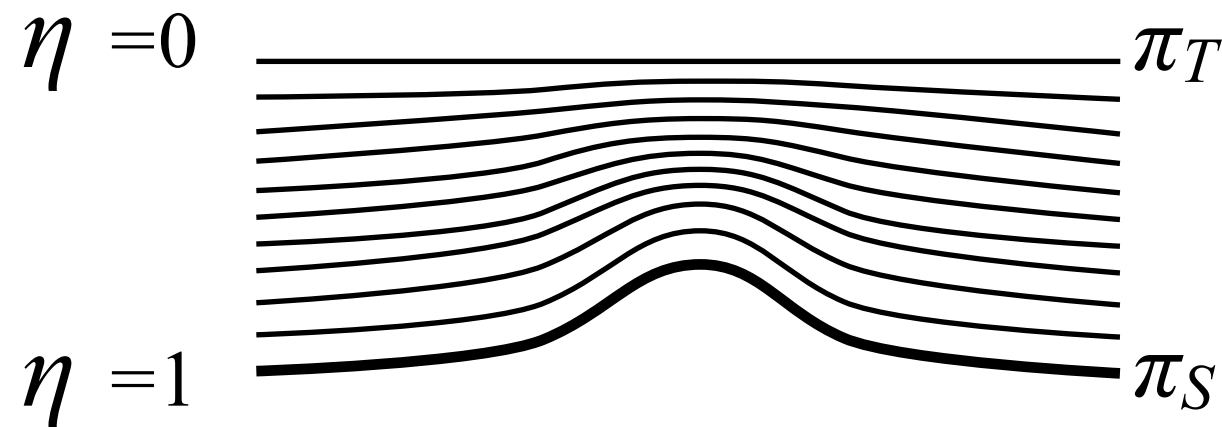
- Arakawa and Lamb (1977)
- Simmons and Burridge (1981)
- Arakawa and Suarez (1983)
- Mesinger and Janjić (1985)
- Janjić (1989)
- ... and many others

The discrete forms of these terms don't necessarily cancel

Terrain-following coordinates

Some other choices

$$\eta = \frac{\pi - \pi_T}{\pi_S - \pi_T} \quad \text{Normalized hydrostatic-pressure}$$



WRF Model
Skamarock and Klemp
(2008)

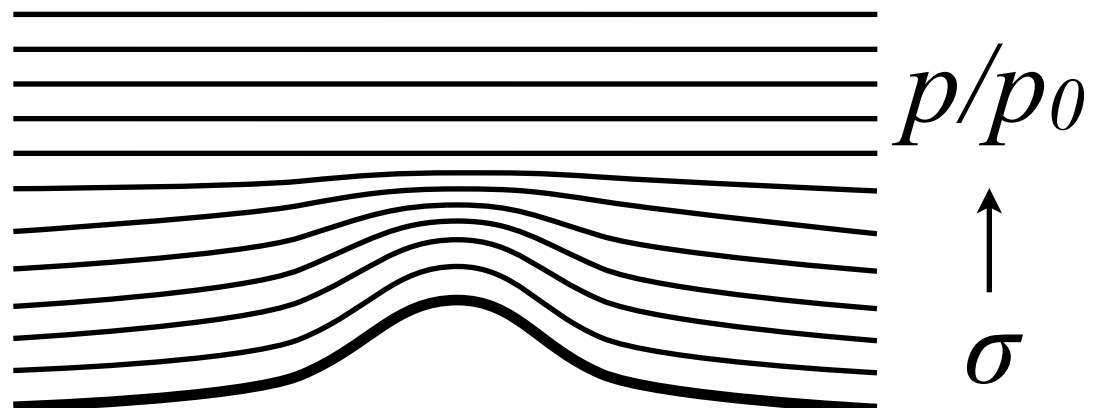
Terrain-following coordinates

Some other choices

Simmons and Burridge (1981)
Hybrid coordinate

$$\eta = \frac{p}{p_s} + \left(\frac{p}{p_s} - 1 \right) \left(\frac{p}{p_s} - \frac{p}{p_0} \right),$$

where $p_0 = \text{constant}$



Terrain-following coordinates

Some other choices

Height-based
coordinates with
vertically-decaying
effects of topography

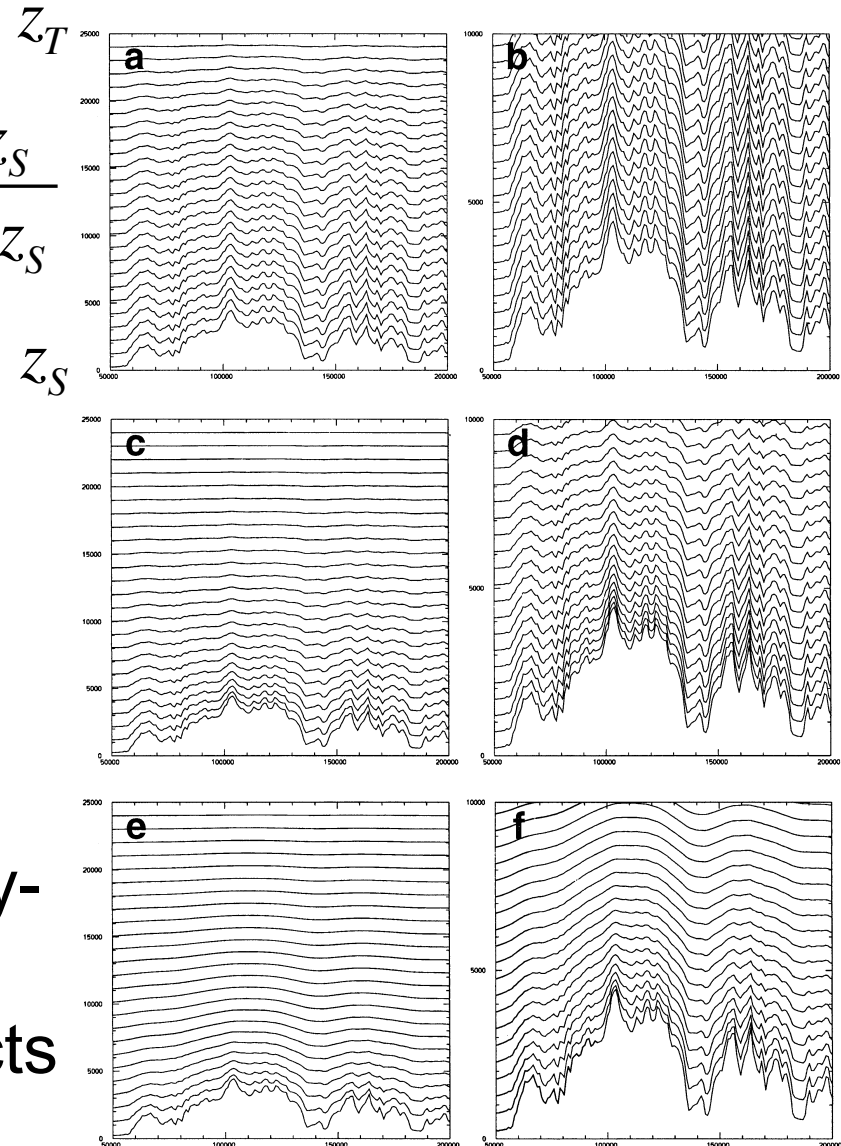
$$\eta = z_T \frac{z - z_S}{z_T - z_S}$$

- Schär et al. (2002)
- Klemp (2011)
(MPAS model --
Skamarock et al. 2012)

Hybrid

Horizontally-
smoothed
terrain effects

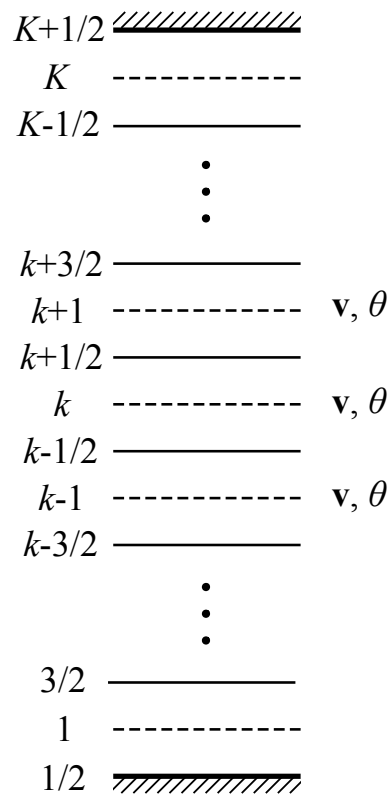
Figure from Schär et al. (2002)



Vertical discretizations

A simple example -- the hydrostatic relation

$$\frac{\partial \phi}{\partial \Pi} = -\theta$$



where

$$\phi = gz$$

$$\Pi = c_p \left(\frac{p}{p_0} \right)^{R/c_p}$$

$$\frac{\phi_{k+1} - \phi_k}{\Pi_{k+1} - \Pi_k} = -\hat{\theta}_{k+1/2} = -\frac{1}{2}(\theta_{k+1} + \theta_k)$$

Averaged

Vertical discretizations

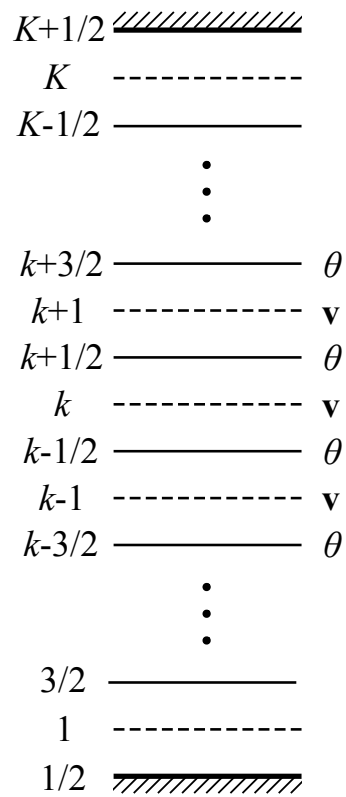
A simple example -- the hydrostatic relation

$$\frac{\partial \phi}{\partial \Pi} = -\theta$$

where

$$\phi = gz$$

$$\Pi = c_p \left(\frac{p}{p_0} \right)^{R/c_p}$$



$$\frac{\phi_{k+1} - \phi_k}{\Pi_{k+1} - \Pi_k} = -\theta_{k+1/2}$$

Theta not averaged

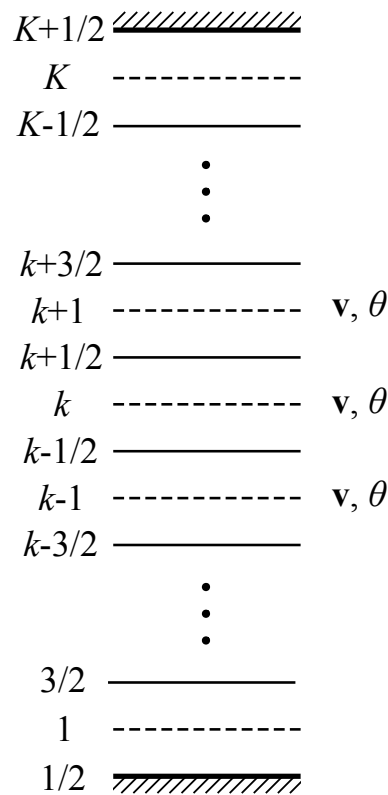
Alternate theta staggering

Vertical discretizations

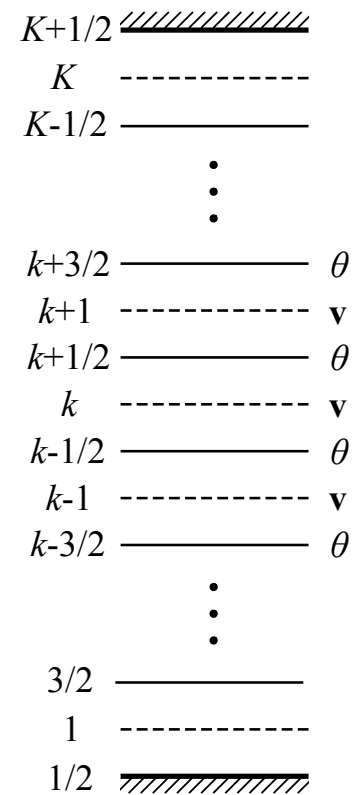
A simple example -- the hydrostatic relation

“A Tale of Two Grids”

Lorenz (“L”) grid



Charney-Phillips
("CP") grid

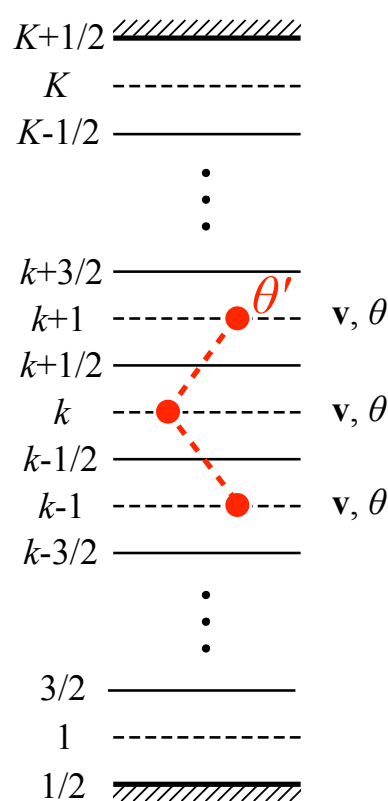


Vertical discretizations

A simple example -- the hydrostatic relation

“A Tale of Two Grids”

Lorenz (“L”) grid



Linearized in p -coordinates:

$$\frac{\phi'_{k+1} - \phi'_k}{\Pi_{k+1} - \Pi_k} = -\frac{1}{2}(\theta'_{k+1} + \theta'_k)$$

We can have

$$\phi'_{k+1} = \phi'_k = 0 \quad \text{if} \quad \theta'_{k+1} = -\theta'_k$$

A non-physical decoupling between the thermal and mass fields, i.e., a computational mode (the dynamics doesn't “feel” the zig-zag in theta)

Vertical discretizations

A simple example -- the hydrostatic relation

“A Tale of Two Grids”

Linearized in p -coordinates:

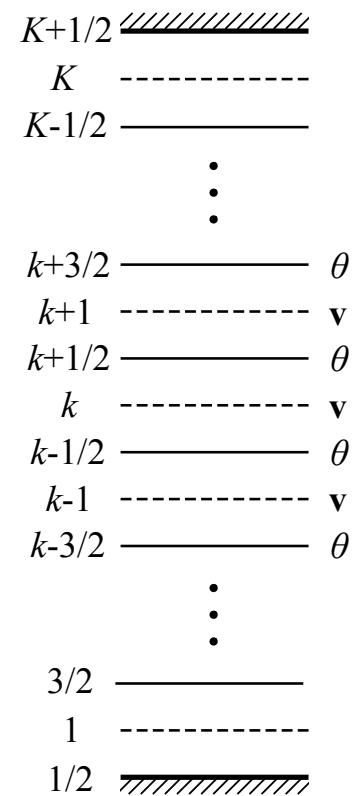
$$\frac{\phi'_{k+1} - \phi'_k}{\Pi_{k+1} - \Pi_k} = -\theta'_{k+1/2}$$

No computational mode supported

See:

- Tokioka (1978)
- Arakawa and Moorthi (1988)
- Arakawa and Konor (1996)

Charney-Phillips (“CP”) grid



Vertical discretizations

There are many possible vertical staggerings and choices of prognostic variables, e.g.,

- for nonhydrostatic system there are 5 prognostic variables
- we can choose any two thermodynamic variables from ρ, p, T, θ , etc.

Some have computational modes, others don't

Vertical discretizations

Accurate representation of waves (acoustic, inertia-gravity, Rossby) best achieved by minimizing vertical averaging and of finite differences over $2\Delta z$

Thuburn and Woollings (2005) analyzed numerical normal-mode solutions of many staggerings, choice of thermodynamic prognostic variables, and three coordinate systems

Vertical discretizations

Example of an optimal configuration (z-coordinates)

Horizontal wavelength = 1000km, $T = 250\text{K}$, Model top at $z = 10\text{km}$

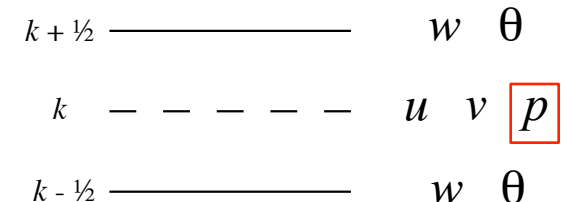
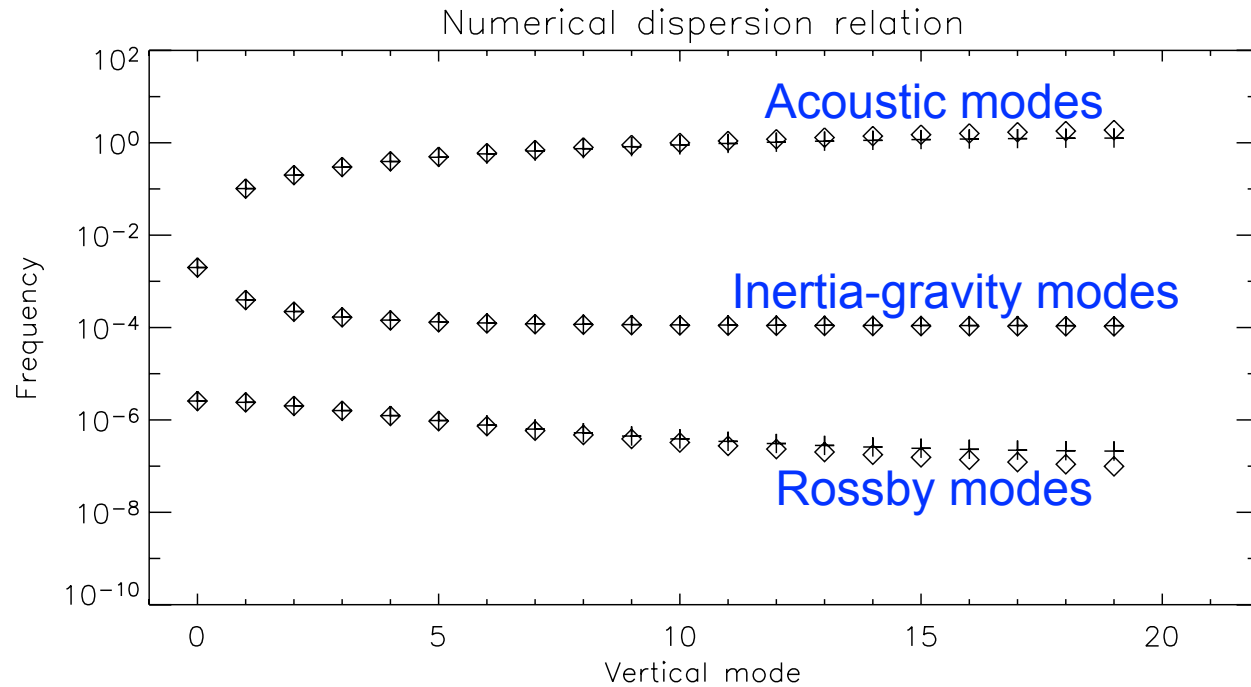


Figure from Thuburn and Woollings (2005)

Diamonds -- continuous solutions
Crosses -- numerical solutions

Vertical discretizations

Example of a sub-optimal configuration (z-coordinates)

Horizontal wavelength = 1000km, $T = 250\text{K}$, Model top at $z = 10\text{km}$

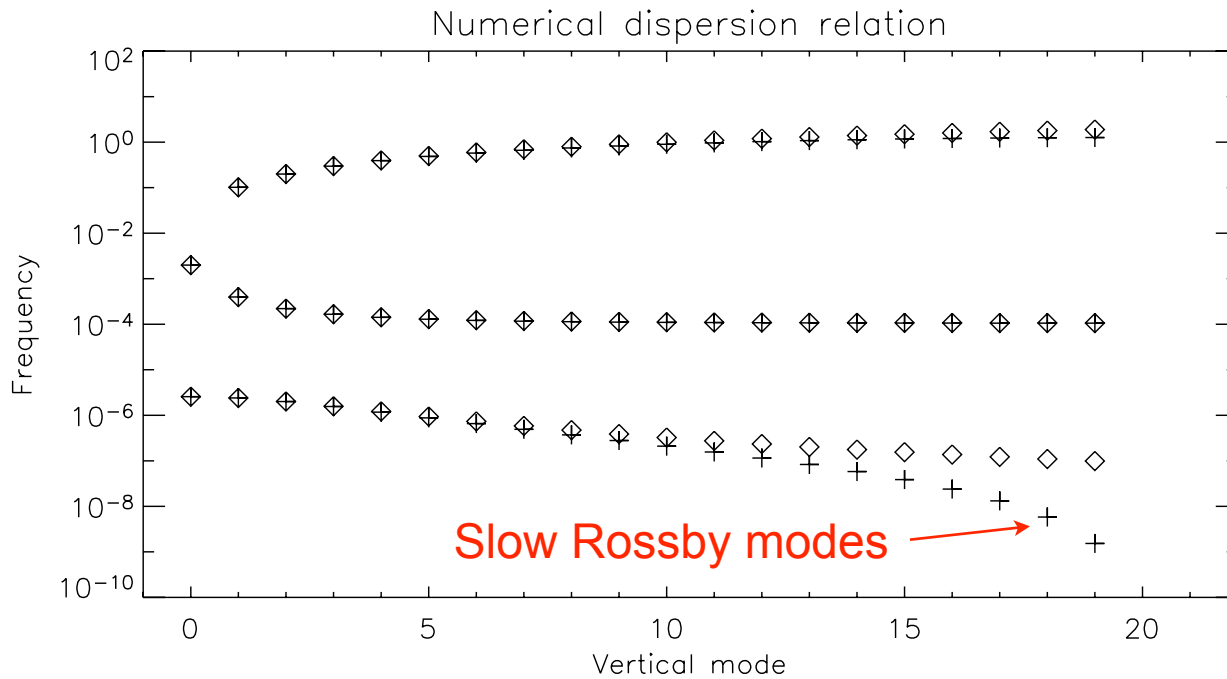
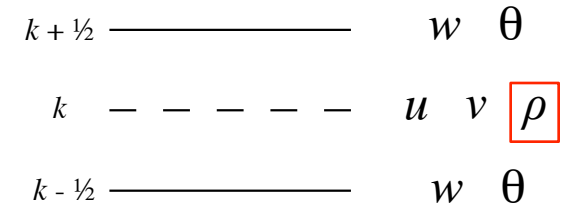


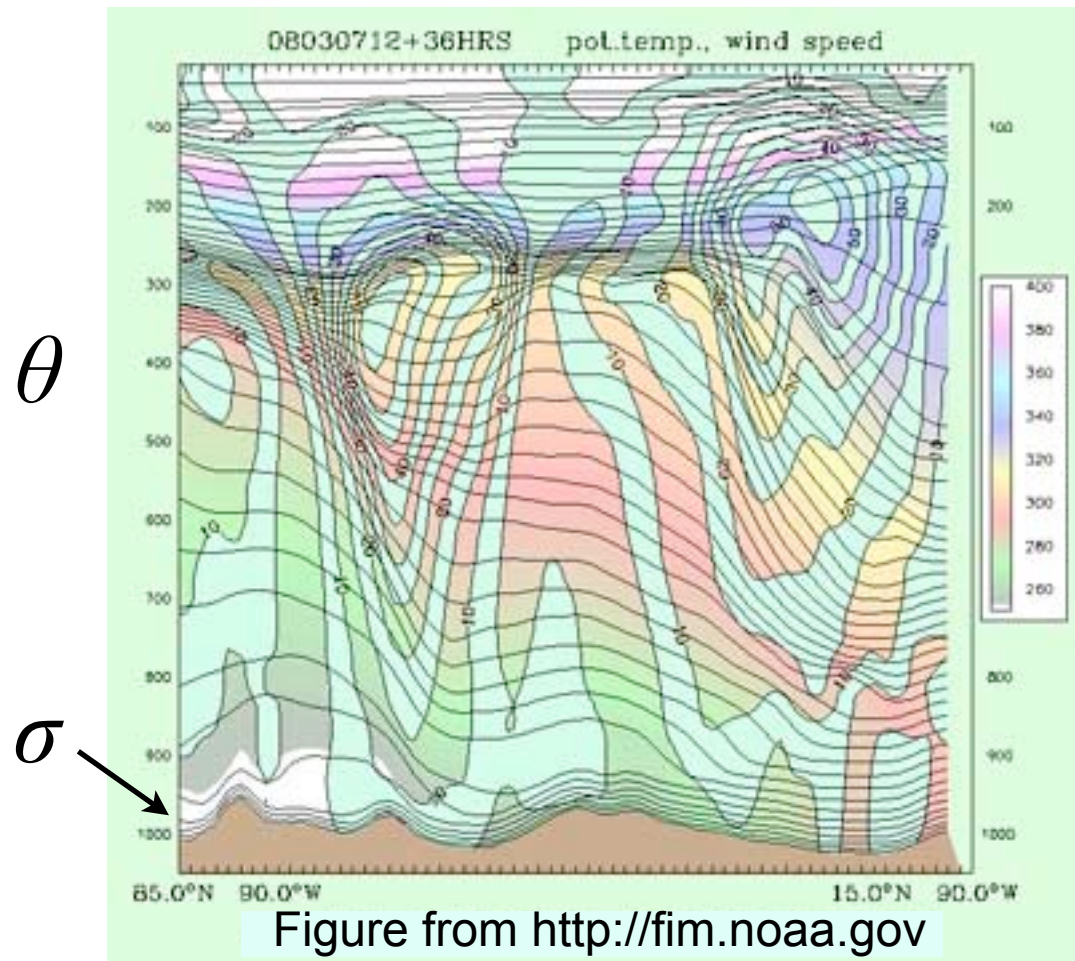
Figure from Thuburn and Woollings (2005)



Note: Thuburn (2006) found that this result is sensitive to the form of the pressure gradient term, i.e., $\frac{1}{\rho} \nabla p$ vs. $\theta \nabla \Pi$

Quasi-Lagrangian vertical coordinates

Often used in a hybrid-coordinate combination with σ
e.g., FIM (Bleck et al. 2010)



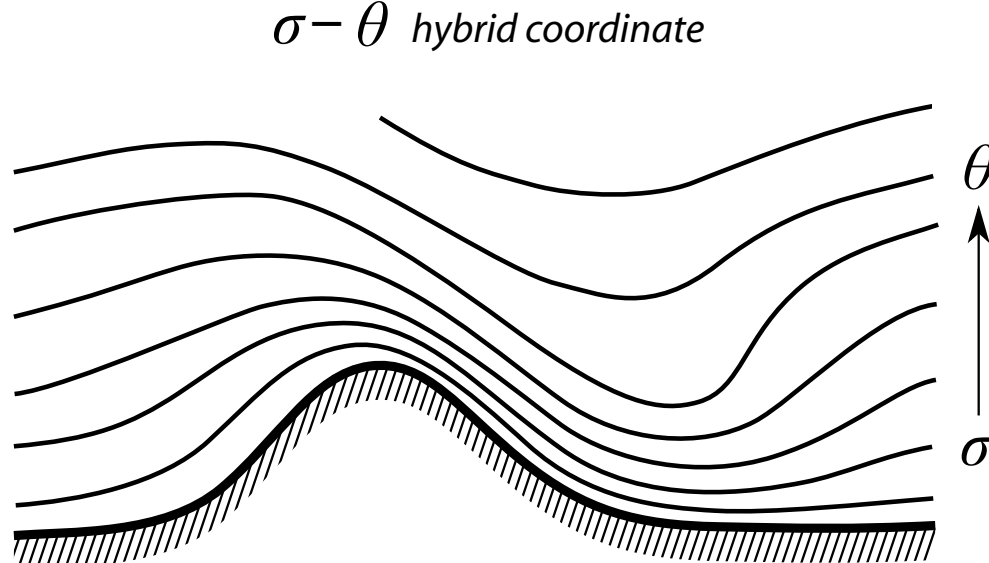
An adaptive grid technique maintains minimum layer thickness constraint through a vertical exchange of mass

Quasi-Lagrangian vertical coordinates

Often used in a hybrid-coordinate combination with σ
e.g., Konor and Arakawa (1997)

$$\eta \equiv F(\sigma, \theta) = f(\sigma) + g(\sigma)\theta$$

where



$$g(\sigma) \rightarrow 0; \quad \left. \begin{array}{l} \sigma \rightarrow \sigma_s \\ \sigma \rightarrow \sigma_t \end{array} \right\}$$
$$f(\sigma) \rightarrow 0, \quad g(\sigma) \rightarrow 1;$$

Quasi-Lagrangian vertical coordinates

Application in nonhydrostatic models:

- Skamarock (1998)
- He (2002)
- Zängl (2007)
- Toy and Randall (2009)
- Toy (2011)

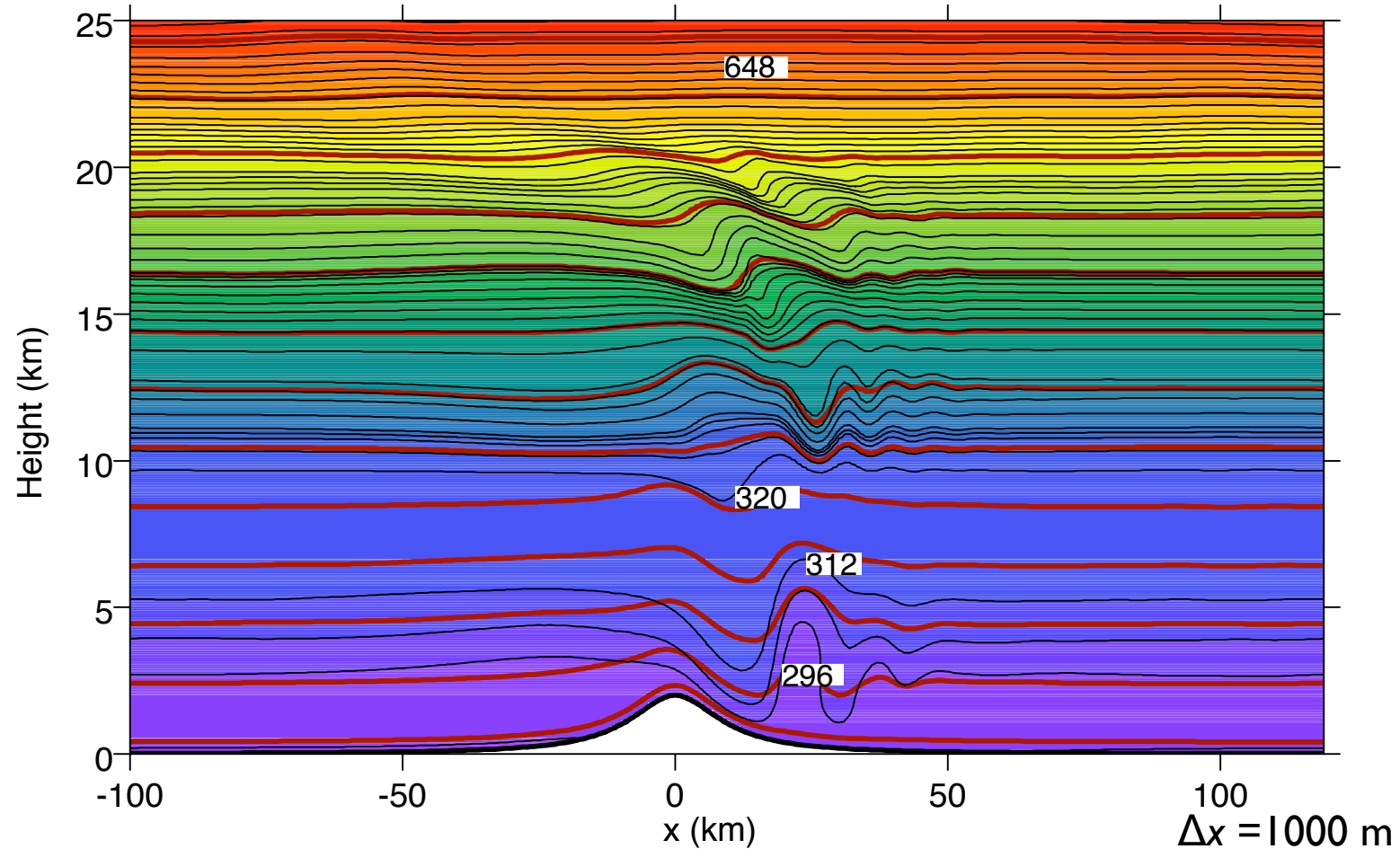


Uses vertical coordinate of Konor and Arakawa (1997) except with the addition of an adaptive grid technique [similar to Arbitrary Lagrangian Eulerian (ALE) methods]

Nonhydrostatic modeling with hybrid isentropic-sigma coordinate

Approach of Toy and Randall (2009) and Toy (2011)

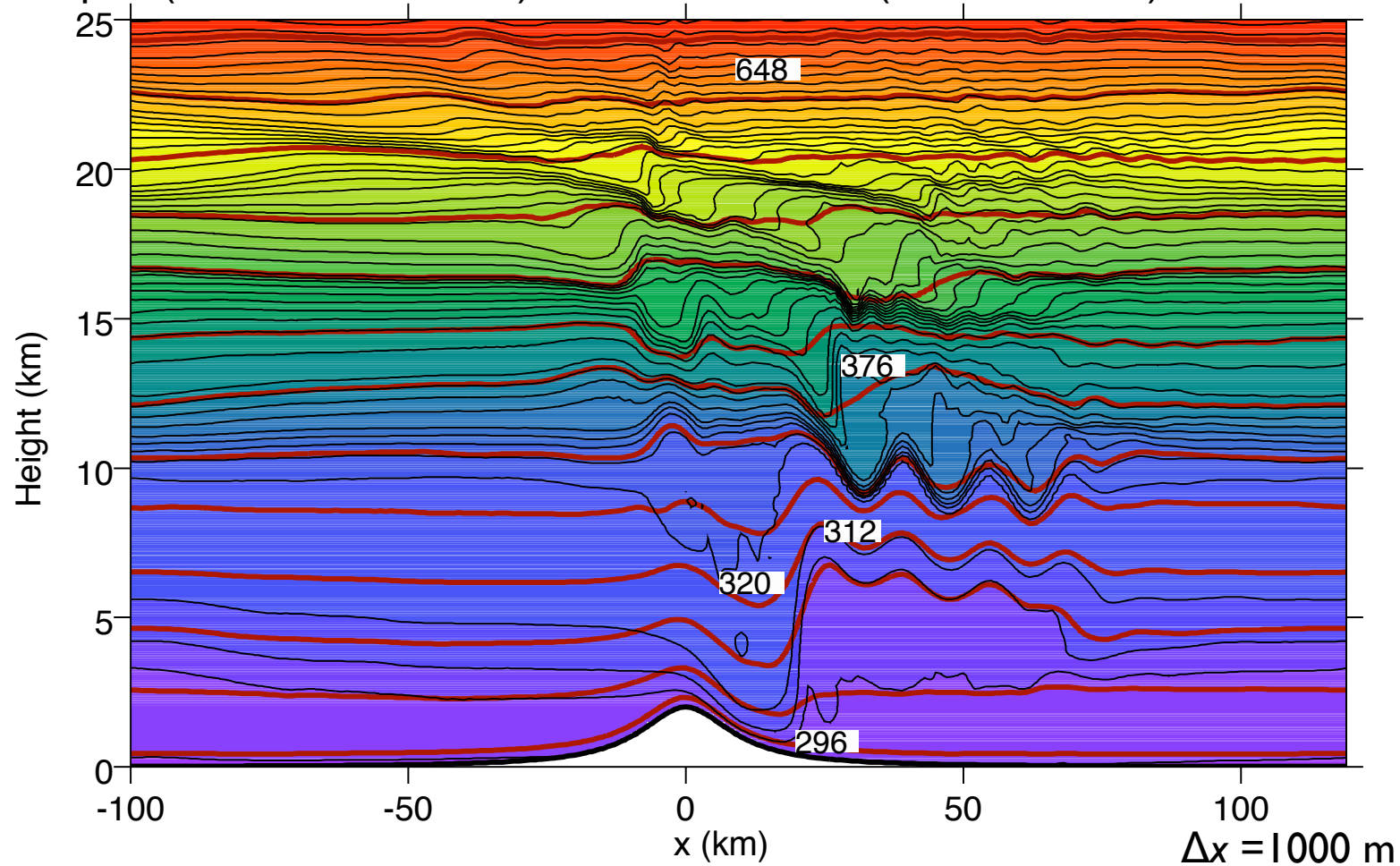
Downslope windstorm simulation -- Boulder, Co -- Jan. 11, 1972
Isentropes (colors+black lines) and model levels (bold red lines) at $t = 70$ min.



Nonhydrostatic modeling with hybrid isentropic-sigma coordinate

Approach of Toy and Randall (2009) and Toy (2011)

Downslope windstorm simulation -- Boulder, Co -- Jan. 11, 1972
Isentropes (colors+black lines) and model levels (bold red lines) at $t = 180$ min.



An aside regarding the generalized vertical velocity $\dot{\eta}$

The model solves the following system in a generalized vertical coordinate (η)

Horizontal momentum $\frac{D\mathbf{v}}{Dt} + f\mathbf{k} \times \mathbf{v} = -\frac{1}{\rho} \nabla_{\eta} p + \frac{1}{m} \frac{\partial p}{\partial \eta} \nabla_{\eta} z$

Vertical momentum $\frac{Dw}{Dt} = -\frac{1}{m} \frac{\partial p}{\partial \eta} - g$

Mass continuity $\left(\frac{\partial m}{\partial t} \right)_{\eta} + \nabla_{\eta} \cdot (m\mathbf{v}) + \frac{\partial}{\partial \eta} (m\dot{\eta}) = 0$

Thermo-dynamic energy $\frac{\partial \theta}{\partial t} + \mathbf{v} \cdot \nabla \theta + \dot{\eta} \frac{\partial \theta}{\partial \eta} = \frac{Q}{\Pi}$

Geopotential energy $\frac{\partial \phi}{\partial t} + \mathbf{v} \cdot \nabla \phi + \dot{\eta} \frac{\partial \phi}{\partial \eta} = wg$

Starr (1945), Lin (2004)
Lagrangian vertical coordinate

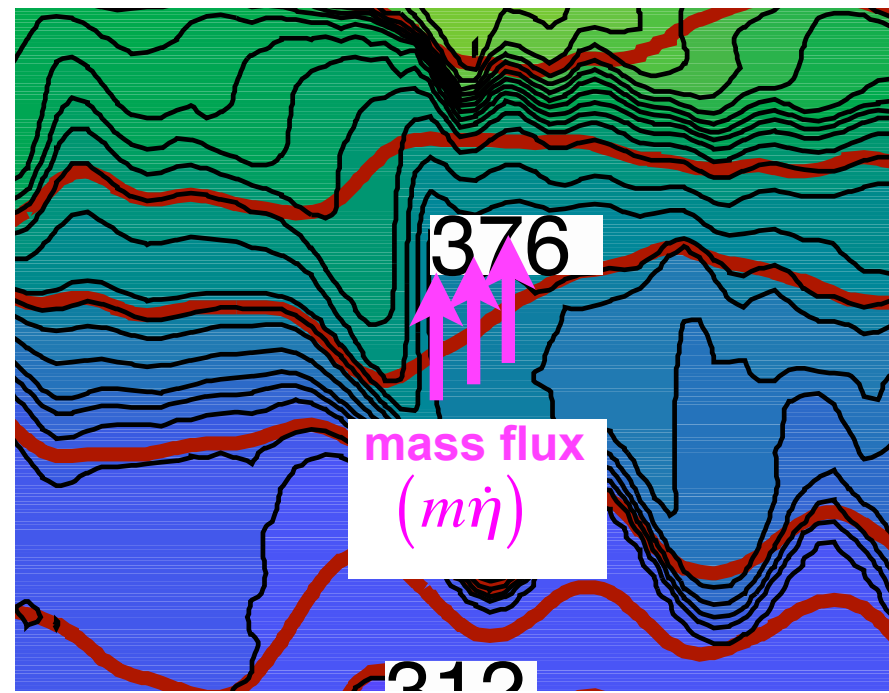
- $\dot{\eta}$ can be arbitrarily specified as long as $\partial z / \partial \eta > 0$ (monotonicity requirement)

- Our goal is to minimize it

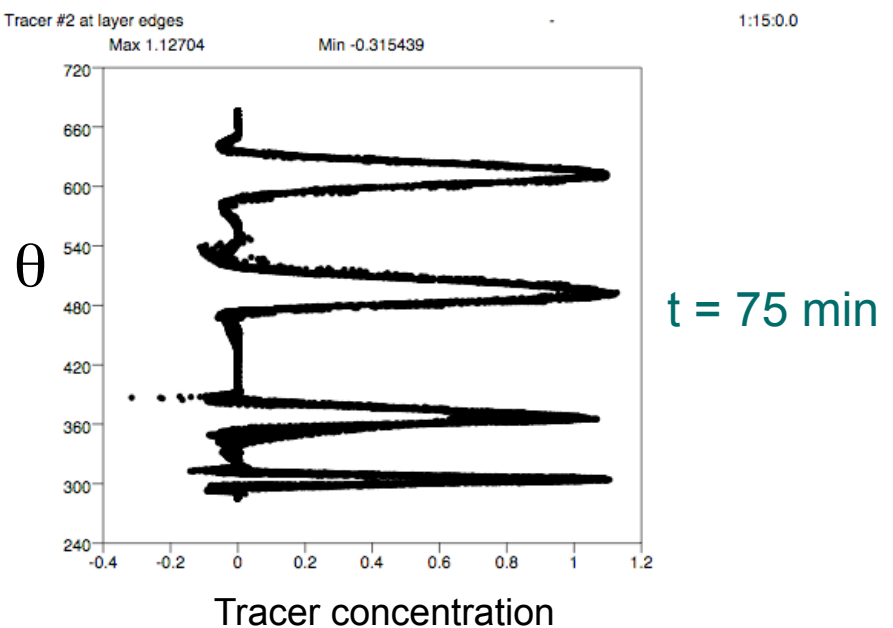
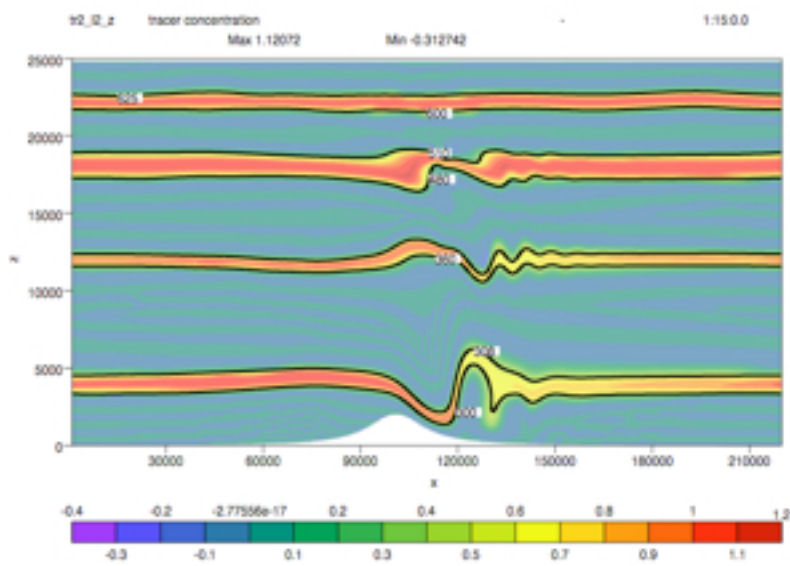
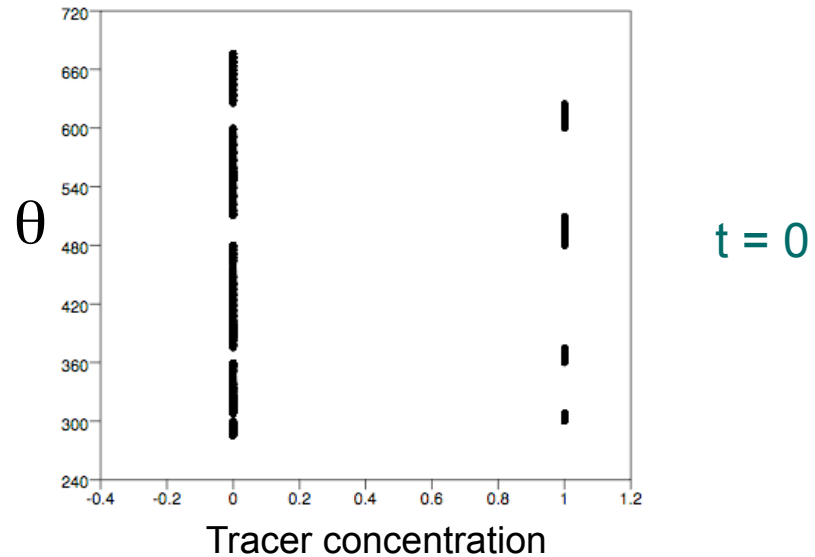
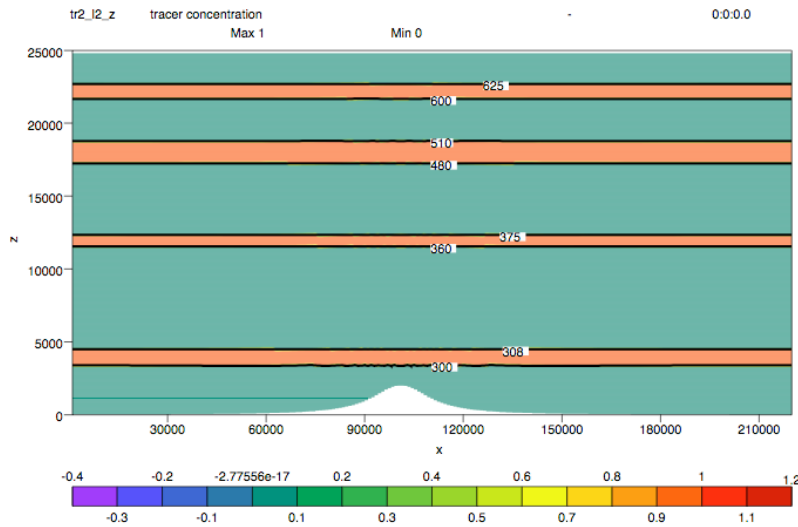
- Note:

- $\dot{\eta} = w$ maintains $\eta = z$
- $\dot{\eta} = \dot{\sigma}$ maintains $\eta = \sigma$
- $\dot{\eta} = \dot{\theta} \approx 0$ maintains $\eta = \theta$
- $\dot{\eta} = \dot{c} \equiv 0$ maintains $\eta = c$

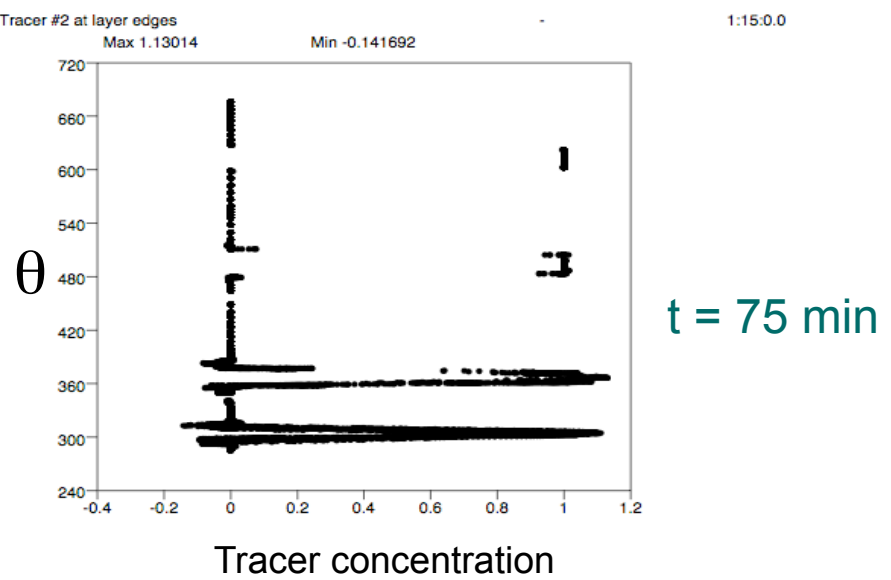
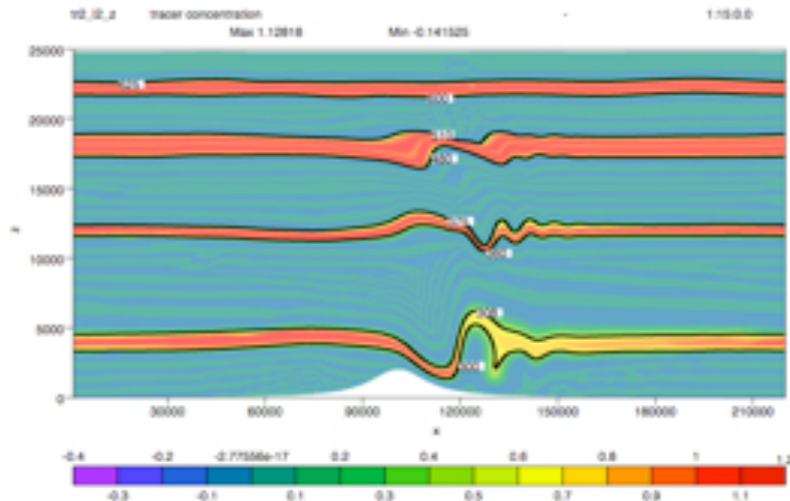
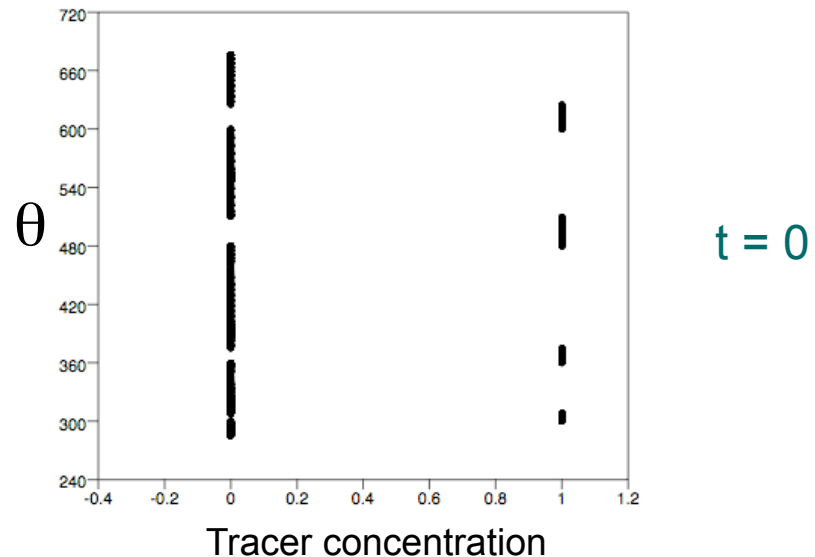
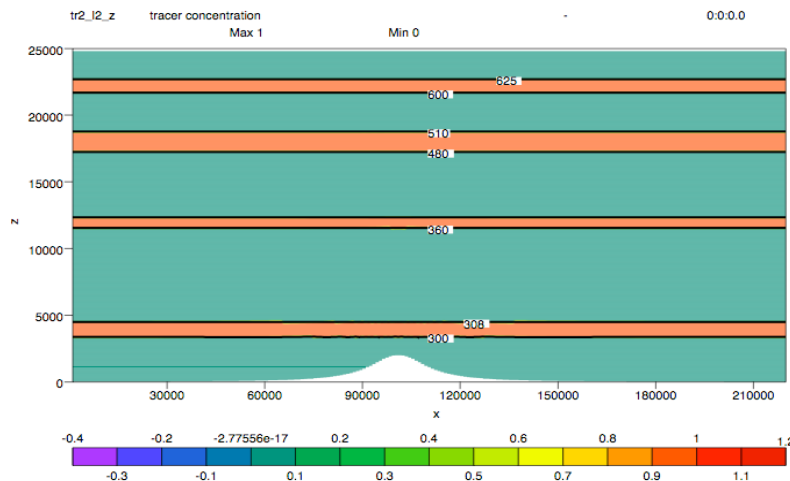
When necessary, flux mass vertically to maintain smooth, evenly spaced coordinate surfaces



Passive tracer advection: Eulerian (σ) vertical coordinate

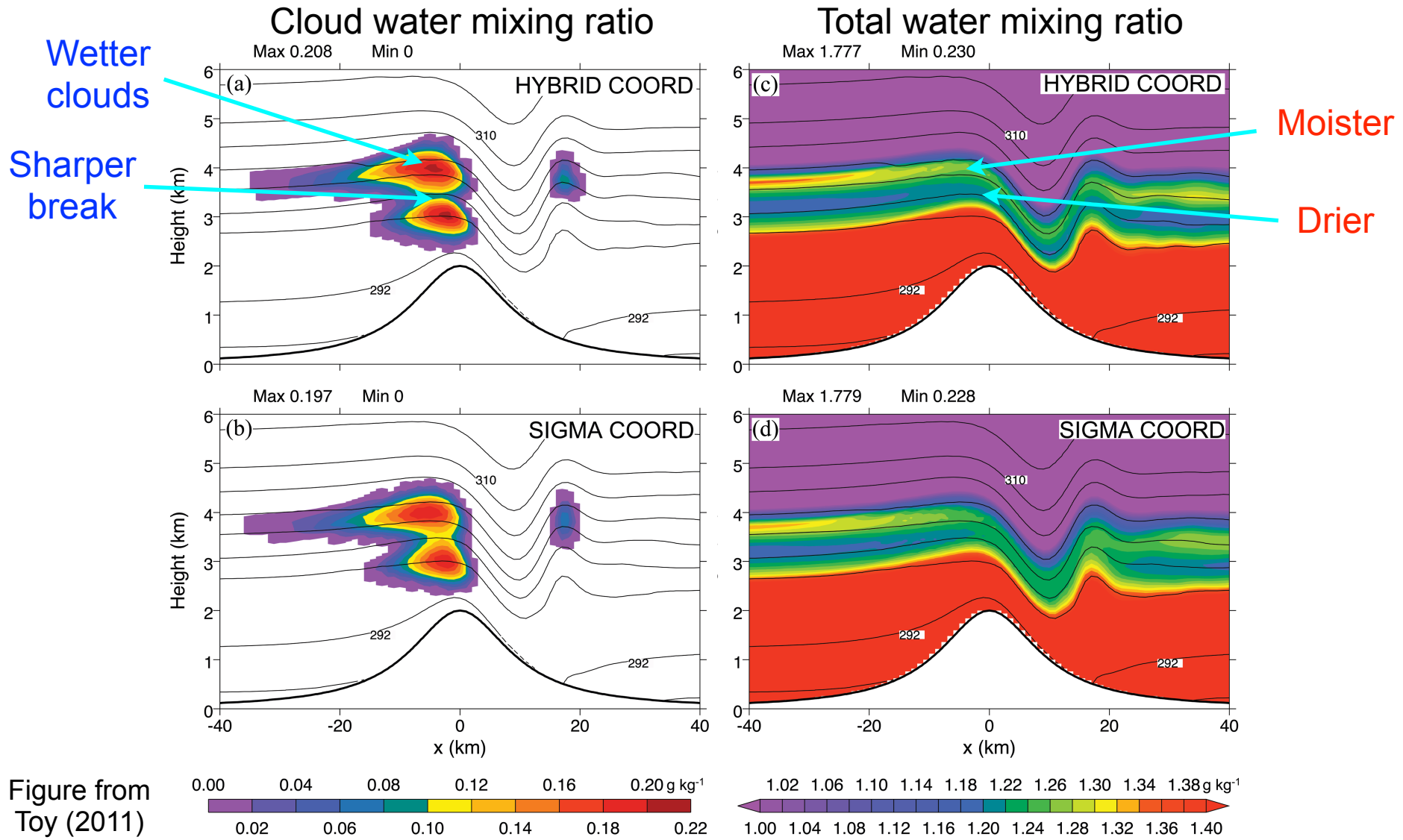


Passive tracer advection: Hybrid vertical coordinate



Wave clouds

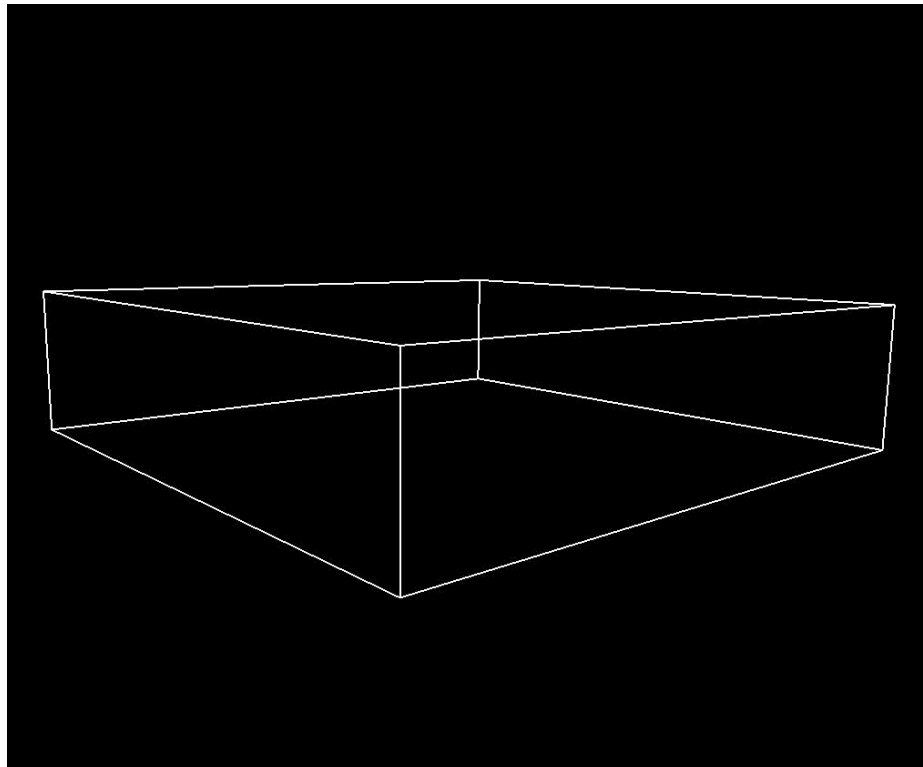
Hybrid vs. sigma coordinates
 $t = 20$ min



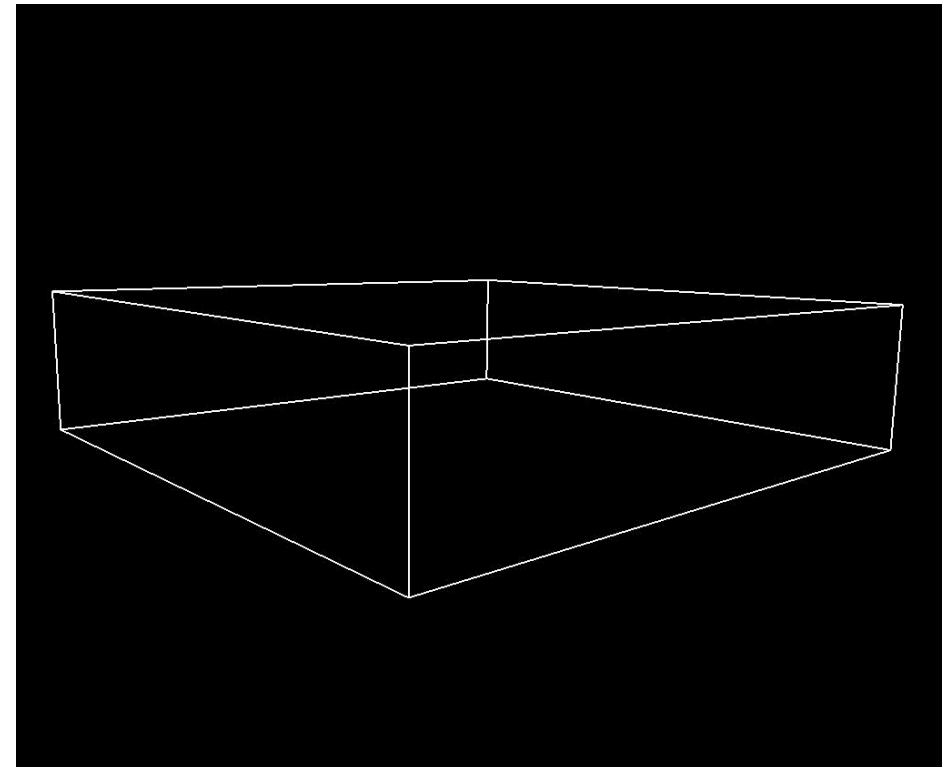
Supercell simulation with nonhydrostatic hybrid-coordinate model

$\Delta x, \Delta y = 1 \text{ km}$

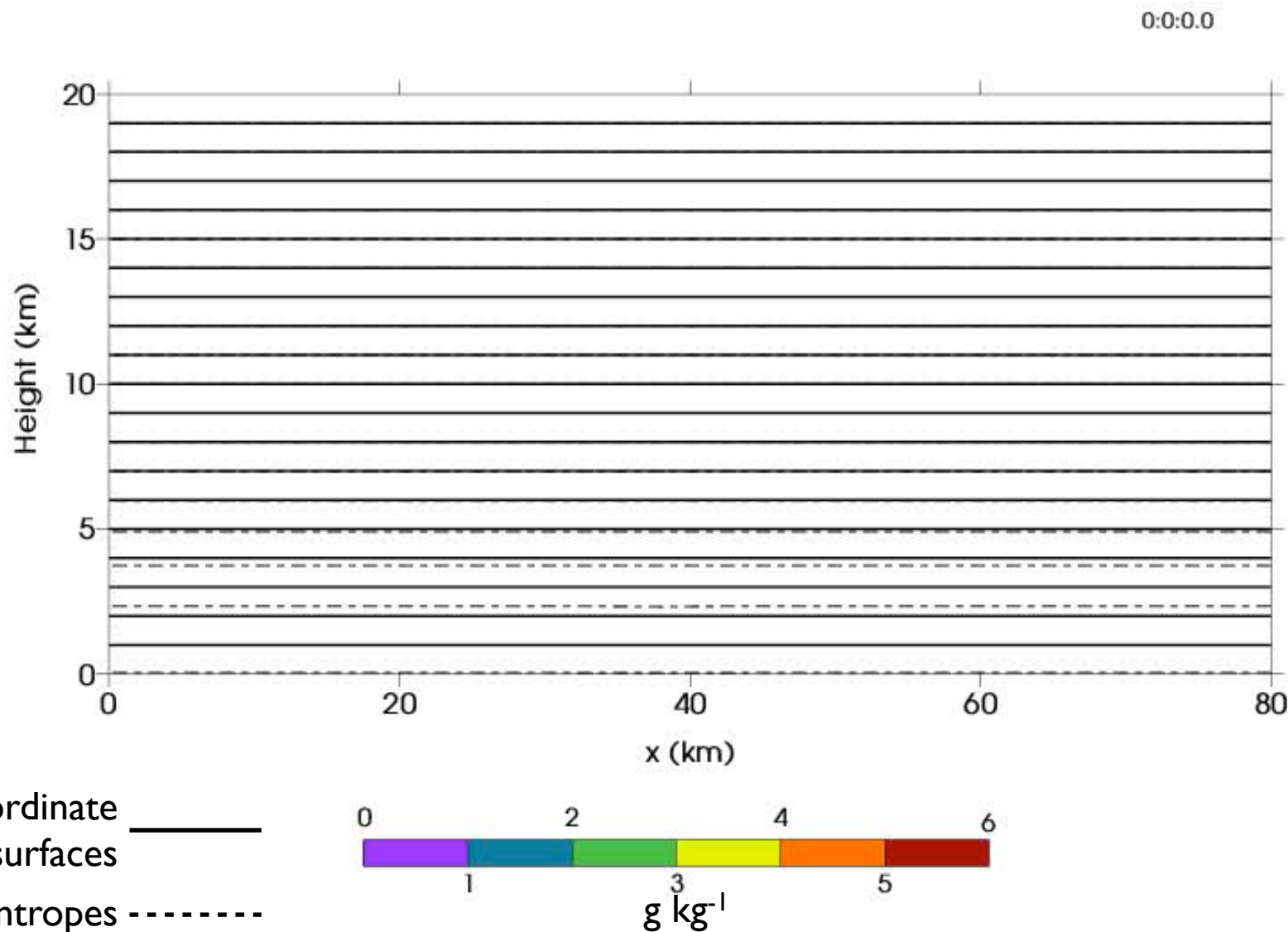
Cloud water



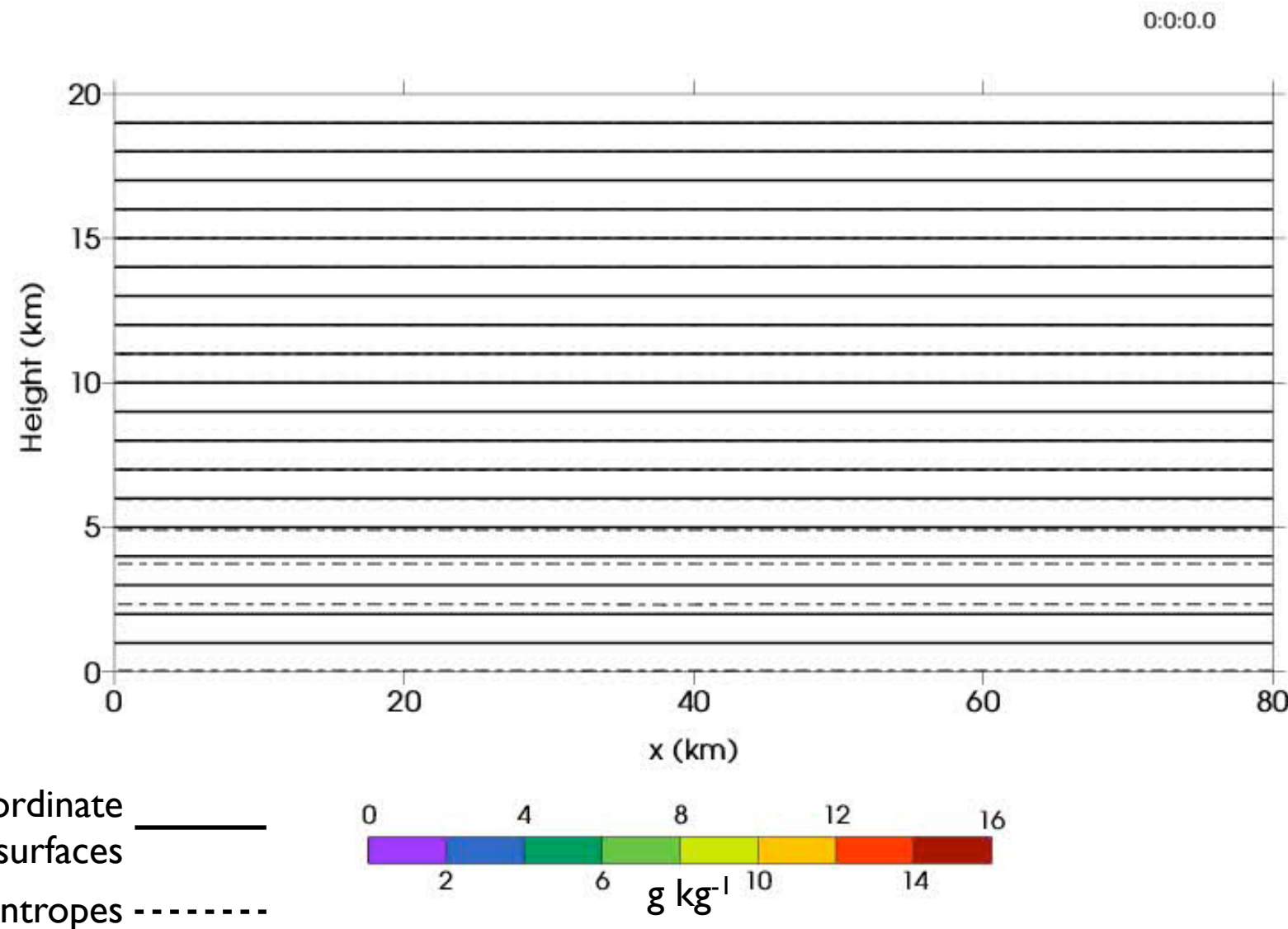
Rain



Vertical slice at $y = 34$ km -- cloud water mixing ratio, theta and hybrid-coordinate levels



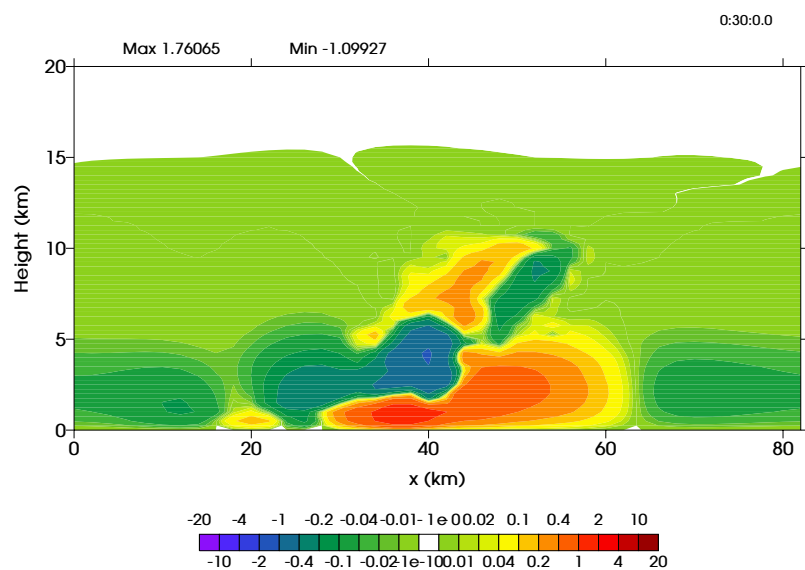
Vertical slice at $y = 34$ km -- rain water mixing ratio, theta and hybrid-coordinate levels



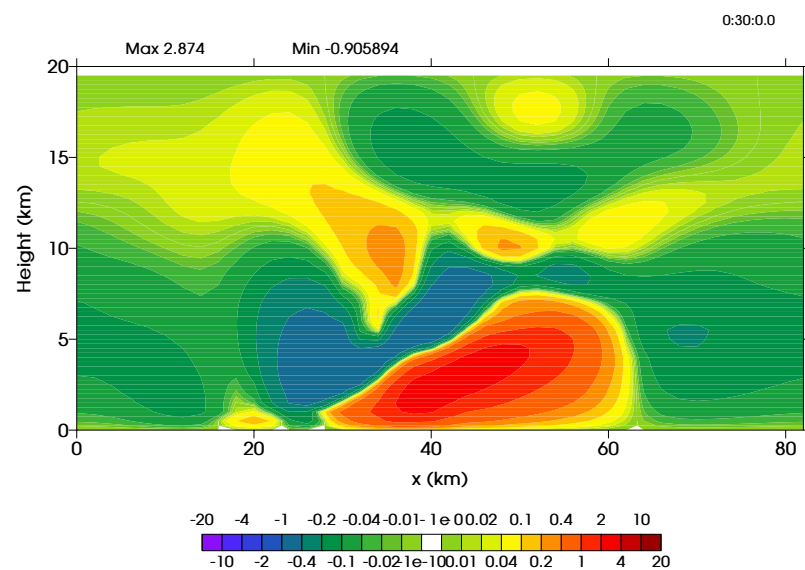
Cross-coordinate mass flux ($\text{kg m}^{-2} \text{ s}^{-1}$) at $y = 34 \text{ km}$

$t = 30 \text{ min}$

Hybrid coord



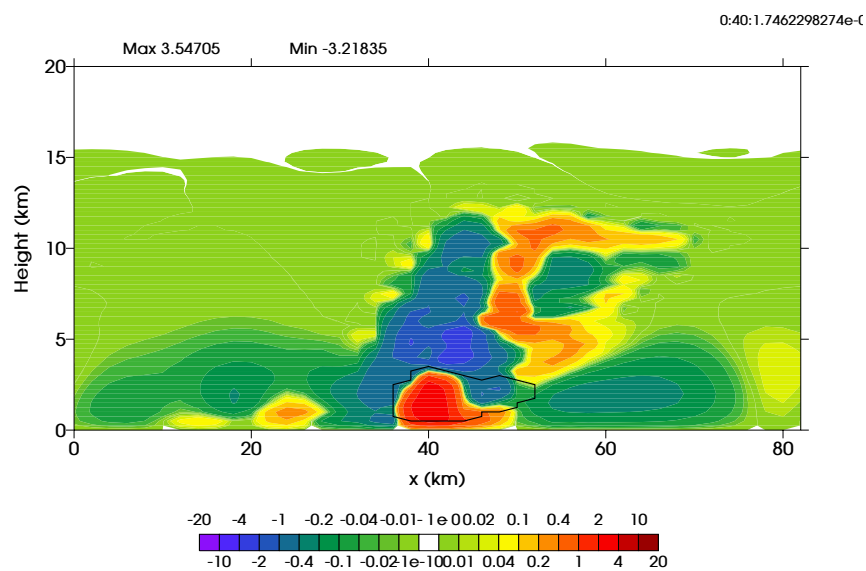
Sigma coord



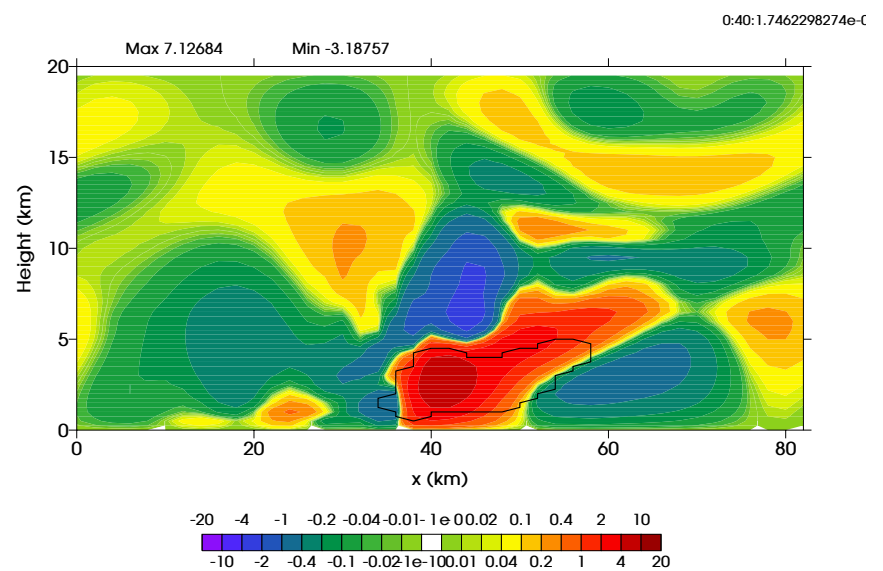
Cross-coordinate mass flux ($\text{kg m}^{-2} \text{ s}^{-1}$) at $y = 34 \text{ km}$

$t = 40 \text{ min}$

Hybrid coord



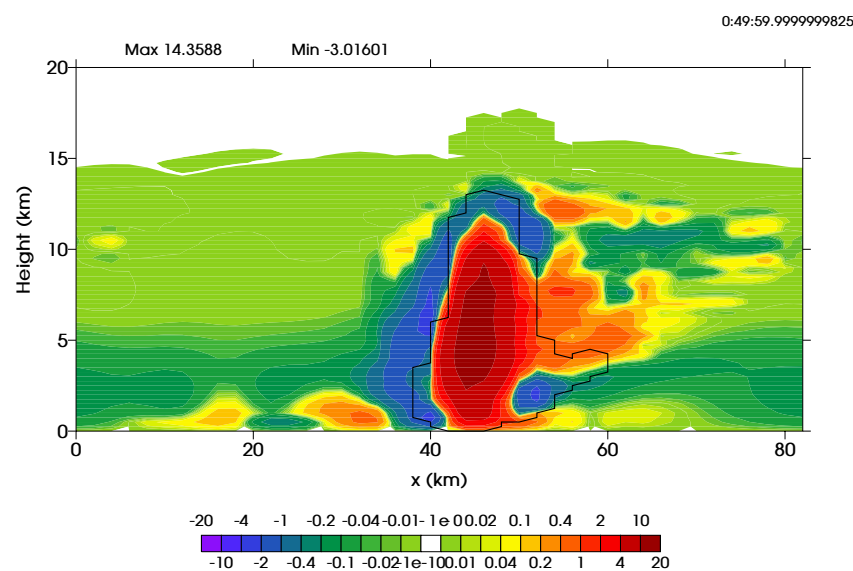
Sigma coord



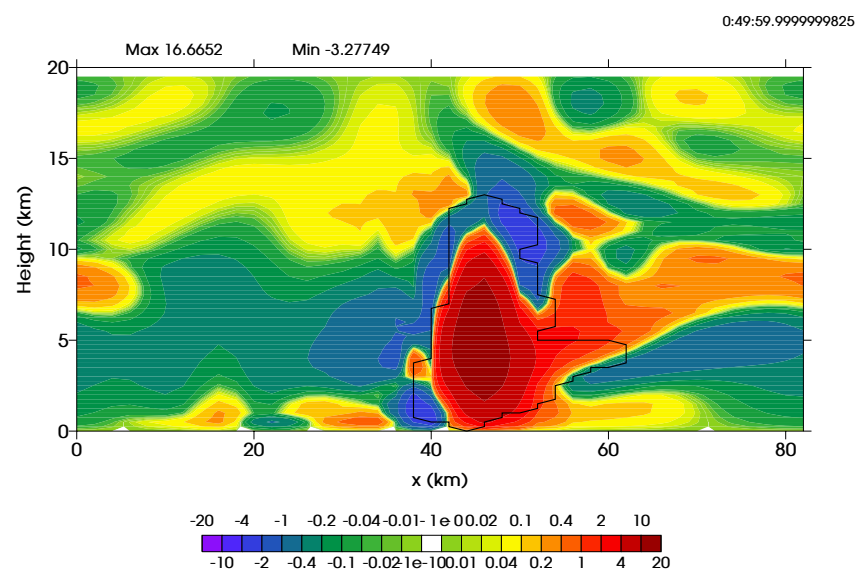
Cross-coordinate mass flux ($\text{kg m}^{-2} \text{ s}^{-1}$) at $y = 34 \text{ km}$

$t = 50 \text{ min}$

Hybrid coord



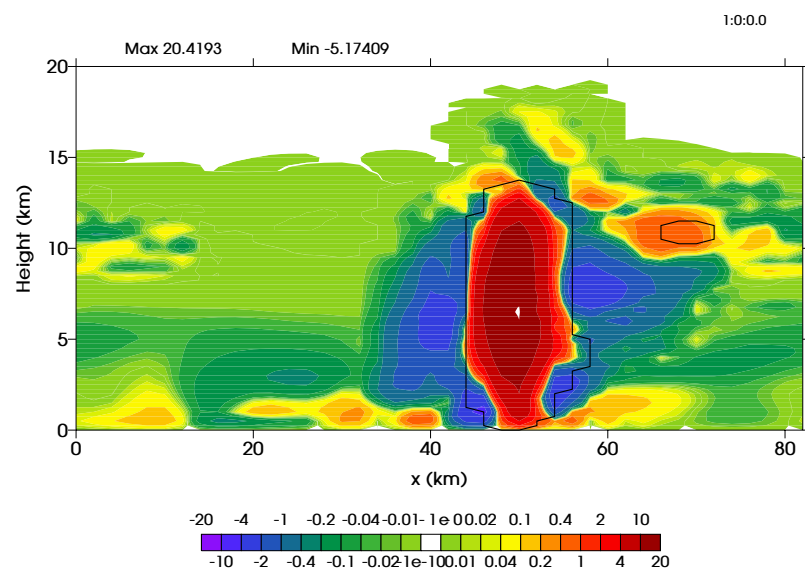
Sigma coord



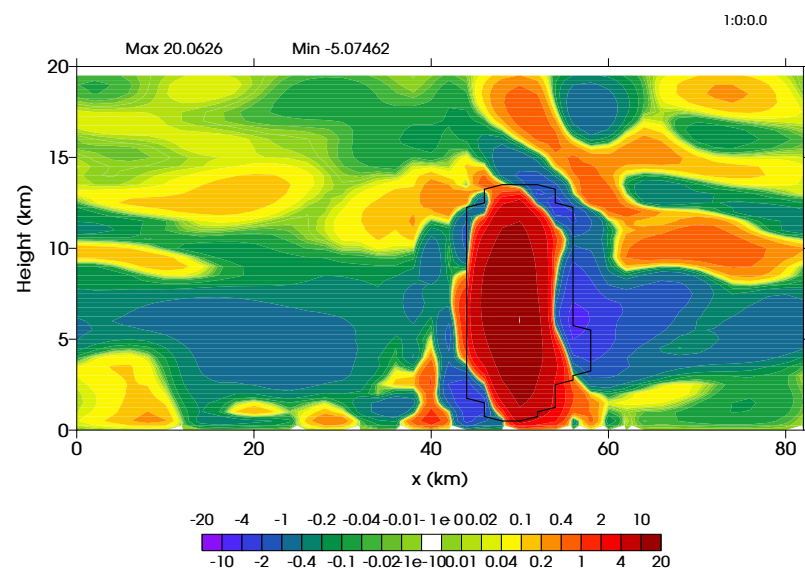
Cross-coordinate mass flux ($\text{kg m}^{-2} \text{ s}^{-1}$) at $y = 34 \text{ km}$

$t = 1 \text{ hr } 00 \text{ min}$

Hybrid coord



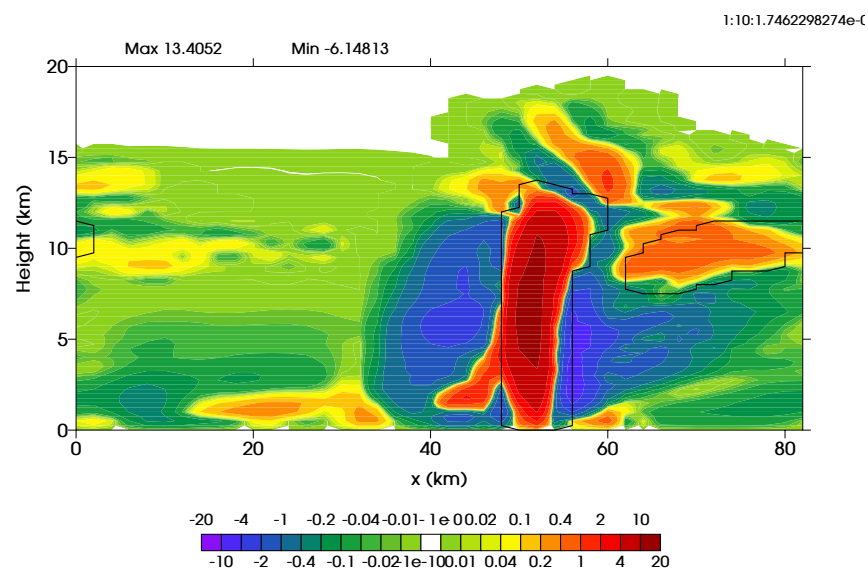
Sigma coord



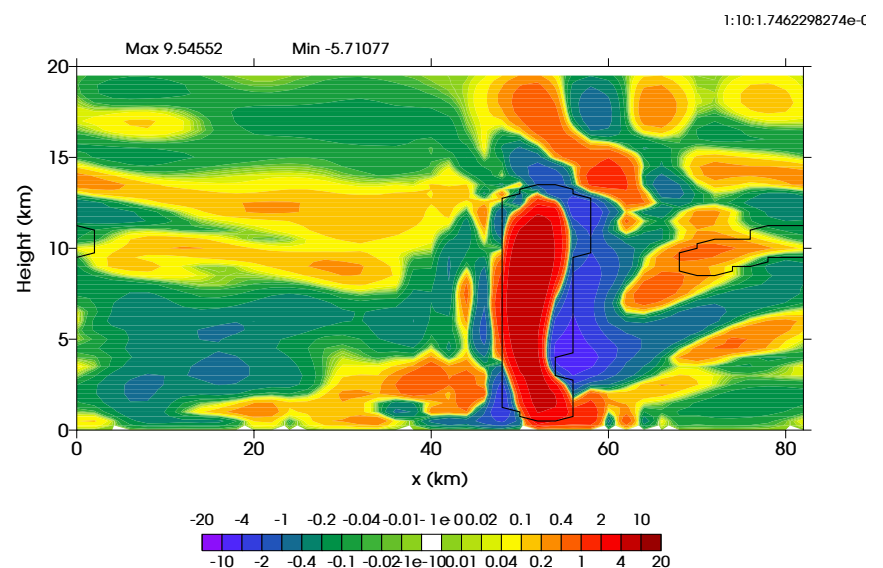
Cross-coordinate mass flux ($\text{kg m}^{-2} \text{ s}^{-1}$) at $y = 34 \text{ km}$

$t = 1\text{hr } 10\text{ min}$

Hybrid coord



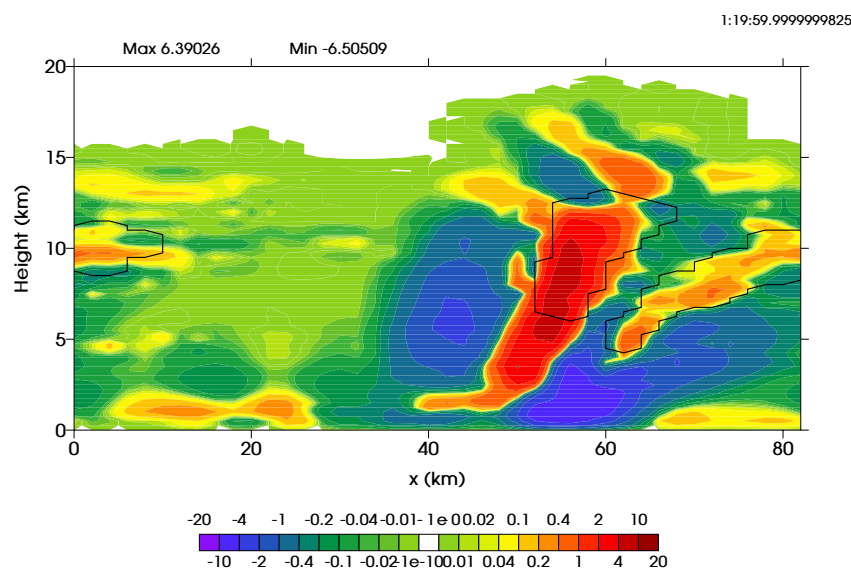
Sigma coord



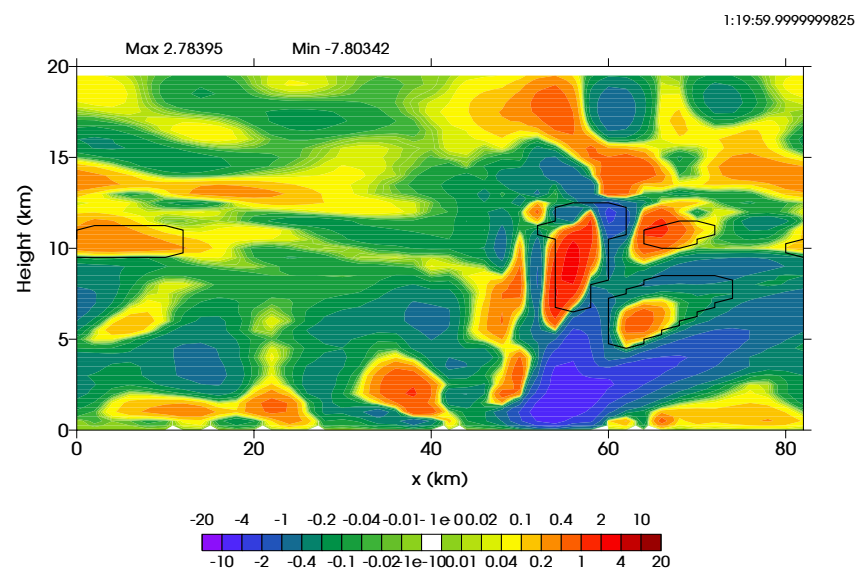
Cross-coordinate mass flux ($\text{kg m}^{-2} \text{ s}^{-1}$) at $y = 34 \text{ km}$

$t = 1 \text{ hr } 20 \text{ min}$

Hybrid coord



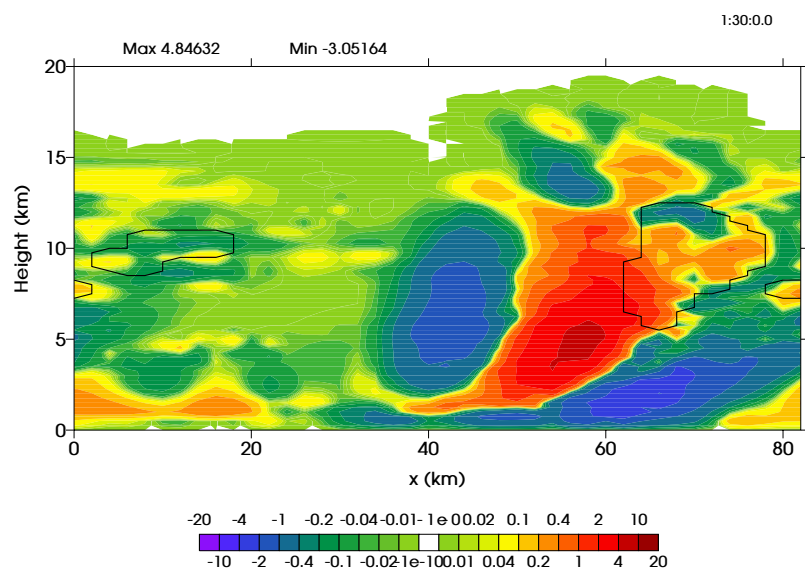
Sigma coord



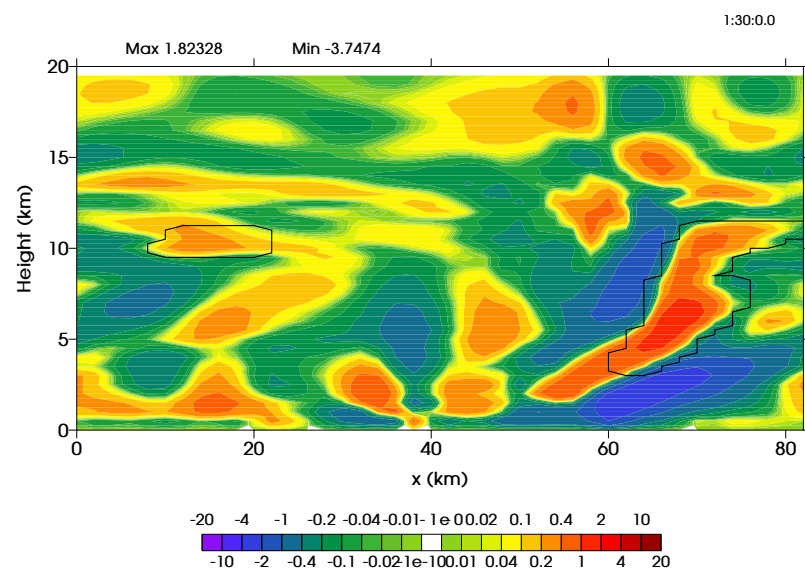
Cross-coordinate mass flux ($\text{kg m}^{-2} \text{ s}^{-1}$) at $y = 34 \text{ km}$

$t = 1 \text{ hr } 30 \text{ min}$

Hybrid coord



Sigma coord



References

- Adcroft, A., C. Hill, and J. Marshall, 1997: Representation of topography by shaved cells in a height coordinate ocean model. *Mon. Wea. Rev.*, **125**, 2293-2315.
- Arakawa, A. and S. Moorthi, 1988: Baroclinic instability in vertically discrete systems. *J. Atmos. Sci.*, **45**, 1688-1707.
- Arakawa, A., and V. Lamb, 1977: Computational design of the basic dynamical processes of the UCLA general circulation model. *Methods in Computational Physics*, Vol. 17, J. Chang, Ed., Academic Press, 173-265.
- Arakawa, A., and M. J. Suarez, 1983: Vertical differencing of the primitive equations in sigma coordinates. *Mon. Wea. Rev.*, **111**, 34-45.
- Arakawa, A. and C. S. Konor, 1996: Vertical differencing of the primitive equations based on the Charney-Phillips grid in hybrid σ - p vertical coordinates. *Mon. Wea. Rev.*, **124**, 511-528.
- Arakawa, A. and S. Moorthi, 1988: Baroclinic instability in vertically discrete systems. *J. Atmos. Sci.*, **45**, 1688-1707.
- Bleck, R., S. Benjamin, J. Lee, and A. E. MacDonald, 2010: On the use of an adaptive, hybrid-isentropic vertical coordinate in global atmospheric modeling. *Mon. Wea. Rev.*, **138**, 2188-2210.

References

- DeMaria, M., 1995: Evaluation of a hydrostatic, height-coordinate formulation of the primitive equations for atmospheric modeling. *Mon. Wea. Rev.*, **123**, 3576-3589.
- Eliassen, A., 1949: The quasi-static equations of motion with pressure as independent variable. *Geofys. Publ.*, **XVII**, 3-44.
- Eliassen, A., and E. Raustein, 1968: A numerical integration experiment with a model atmosphere based on isentropic coordinates. *Meteorologiske Annaler*, **5**(2), 45-63.
- He, Z., 2002: A non-hydrostatic model with a generalized vertical coordinate. Ph.D. thesis, University of Miami, 99 pp.
- Janjić, Z. I., 1989: On the pressure gradient force error in σ -coordinate spectral models. *Mon. Wea. Rev.*, **117**, 2285-2292.
- Kasahara, A. and W. M. Washington, 1967: NCAR global general circulation model of the atmosphere. *Mon. Wea. Rev.*, **95**, 389-402.
- Kasahara, A., 1974: Various vertical coordinate systems used for numerical weather prediction. *Mon. Wea. Rev.*, **102**, 509-522.
- Klemp, J. B., 2011: A terrain-following coordinate with smoothed coordinate surfaces. *Mon. Wea. Rev.*, **139**, 2163-2169.

References

- Konor, C. S., and A. Arakawa, 1997: Design of an atmospheric model based on a generalized vertical coordinate. *Mon. Wea. Rev.*, **125**, 1649-1673.
- Laprise, R., 1992: The Euler equations of motion with hydrostatic pressure as an independent variable. *Mon. Wea. Rev.*, **120**, 197-207.
- Lin, S.-J., 2004: A “vertically Lagrangian” finite-volume dynamical core for global models. *Mon. Wea. Rev.*, **132**, 2293-2307.
- Lock, S.-J., H.-W. Bitzer, A. Coals, A. Gadian and S. Mobbs, 2012: Demonstration of a cut-cell representation of 3D orography for studies of atmospheric flows over very steep hills. *Mon. Wea. Rev.*, **140**, 411-424.
- Mesinger, F., and Z. I. Janjić, 1985: Problems and numerical methods of the incorporation of mountains in atmospheric models. *Large-Scale Computations in Fluid Mechanics*, Part 2. Lec. Appl. Math., Vol. 22, Amer. Math. Soc., 81-120.
- Phillips, N. A., 1957: A coordinate system having some special advantages for numerical forecasting. *J. Meteor.*, **14**, 184-185.
- Richardson, L. F., 1922: *Weather Prediction by Numerical Process*. Cambridge University Press, 236 pp.

References

- Schär, C., D. Leuenberger, O. Fuhrer, D. Lüthi, and C. Girard, 2002: A new terrain-following vertical coordinate formulation for atmospheric prediction models. *Mon. Wea. Rev.*, **130**, 2459-2480.
- Simmons, A. J., and D. M. Burridge, 1981: An energy and angular-momentum conserving vertical finite-difference scheme and hybrid vertical coordinates. *Mon. Wea. Rev.*, **109**, 758-766.
- Skamarock, W. C., 1998: A hybrid-coordinate nonhydrostatic model. Preprints, *12th Conf. on Numerical Weather Prediction*, Phoenix, AZ, Amer. Meteor. Soc., 232-235.
- Skamarock, W. C. and J. B. Klemp, 2008: A time-split nonhydrostatic atmospheric model for weather research and forecasting applications. *J. Comput. Phys.*, **227**, 3465-3485.
- Skamarock, W. C., J. B. Klemp, M. G. Duda, L. D. Fowler, S.-H. Park, and T. D. Ringler, 2012: A multi-scale nonhydrostatic atmospheric model using centroidal voronoi tessellations and C-grid staggering. *Mon. Wea. Rev.* doi: 10.1175/MWR-D-11-00215.1, in press.
- Starr, V. P., 1945: A quasi-Lagrangian system of hydrodynamical equations. *J. Meteor.*, **2**, 227-237.

References

- Steppeler, J., H.-W. Bitzer, M. Minotte, and L. Bonaventura, 2002: Nonhydrostatic atmospheric modeling using a z-coordinate representation, *Mon. Wea. Rev.*, **130**, 2143-2149.
- Thuburn, J., 2006: Vertical discretizations giving optimal representation of normal modes: Sensitivity to the form of the pressure-gradient term. *Quart. J. Roy. Meteor. Soc.*, **132**, 2809-2825.
- Thuburn, J., and T. J. Woollings, 2005: Vertical discretizations for compressible Euler equation atmospheric models giving optimal representation of normal modes. *J. Comput. Phys.*, **203**, 386-404.
- Tokioka, T., 1978: Some considerations on vertical differencing. *J. Meteor. Soc. Japan*, **56**, 98-111.
- Toy, M. D., 2011: Incorporating condensational heating into a nonhydrostatic atmospheric model based on a hybrid isentropic-sigma vertical coordinate. *Mon. Wea. Rev.*, **139**, 2940-2954.
- Toy, M. D., and D. A. Randall, 2009: Design of a nonhydrostatic atmospheric model based on a generalized vertical coordinate. *Mon. Wea. Rev.*, **137**, 2305-2330.
- Walko, R. L. and R. Avissar, 2008: The ocean-land-atmosphere model (OLAM). Part II: Formulation and tests of the nonhydrostatic dynamic core. *Mon. Wea. Rev.*, **136**, 4045-4062.

References

- Yamazaki, H. and T. Satomura, 2010: Nonhydrostatic atmospheric modeling using a combined cartesian grid. *Mon. Wea. Rev.*, **138**, 3932-3945.
- Zängl, G., 2007: An adaptive vertical coordinate formulation for a nonhydrostatic model with flux-form equations. *Mon. Wea. Rev.*, **135**, 228-239.